Ann. Comb. 25 (2021) 345–392

Published online April 16, 2021
https://doi.org/10.1007/s00026-021-00531-w

Annals of Combinatorics

Non-crossing Trees, Quadrangular Dissections, Ternary Trees, and Duality-Preserving Bijections

Nikos Apostolakis

Abstract. Using the theory of Properly Embedded Graphs developed in an earlier work we define an involutory duality on the set of labeled non-crossing trees that lifts the obvious duality in the set of unlabeled non-crossing trees. The set of non-crossing trees is a free ternary magma with one generator and this duality is an instance of a duality that is defined in any such magma. Any two free ternary magmas with one generator are isomorphic via a unique isomorphism that we call the structural bijection. Besides the set of non-crossing trees we also consider as free ternary magmas with one generator the set of ternary trees, the set of quadrangular dissections, and the set of flagged Perfectly Chain Decomposed Ditrees, and we give topological and/or combinatorial interpretations of the structural bijections between them. In particular the bijection from the set of quadrangular dissections to the set of non-crossing trees seems to be new. Further we give explicit formulas for the number of self-dual labeled and unlabeled non-crossing trees and the set of quadrangular dissections up to rotations and up to rotations and reflections.

1. Introduction

This paper follows [1] as the second in a planned series that explore the theory and applications of *Properly Embedded Graphs* (*pegs*) and their duality. The

The Computer Algebra Systems Sage [7] and GAP [11] were used extensively to confirm calculations and check conjectures at several stages of this project. I would like to thank Cormac O'Sullivan for valuable comments. Finally, I would also like to thank the referees of this and earlier versions of the paper for invaluable comments and for suggesting interesting connections with the literature.

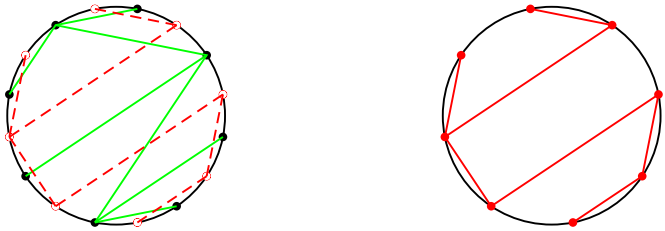

FIGURE 1. An unlabeled non-crossing tree and its dual

main motivation is to understand duality of non-crossing trees and in particular to enumerate the set of self-dual objects. This leads to a more broad investigation of duality in Fuss–Catalan objects for $p = 3$.[1]

Non-crossing trees are well studied in the literature, see for example [8], and [22]. A *non-crossing tree* is a tree with vertices on a circle, typically at the vertices of a regular polygon, and edges mutually non-intersecting chords. Usually the vertices are labeled $1, \ldots, n$, where n is the number of vertices, and if this is not the case we will talk of *unlabeled* non-crossing trees. There is a topologically obvious way to define the dual of an unlabeled non-crossing tree t: removing the tree breaks the circle into arcs and the interior of the circle into simply connected regions, and there is exactly one arc in the boundary of each region. The dual t^* is defined by putting a vertex in each arc and connecting two of these vertices by an edge if and only if the corresponding regions share an edge. Clearly t^* is non-crossing and $(t^*)^* = t$; for an example of this construction see Fig. 1. We call this duality *nc-duality*.

Lifting nc-duality to an *involutory* duality at the level of labeled non-crossing trees is not straightforward, and it involves clarifying some subtle issues that have to do with the orientation of the circle. For example a "duality" for labeled non-crossing trees was defined in [15] by labeling the dual vertex that follows i in the standard (counterclockwise) orientation of the circle by i, as in Fig. 2. Clearly this operation is not involutory, rather it has order $2n$ where n is the number of vertices of the tree. For this reason we call the resulting tree the *complement*, rather than the *dual*, of t and denote it by $\kappa(t)$, since as we will see in Sect. 2.5.2 it is induced by the *Kreweras complement* in the lattice of non-crossing partitions.

From the point of view of [1][2], non-crossing trees are trees *properly embedded* in the disk, and nc-duality in the unlabeled case is simply the *mind-body duality*[3]. One could then use mind-body duality for labeled pegs to lift nc-duality to labeled non-crossing trees. This approach however, has the drawback that the mind-body dual t^* of a peg is embedded in the oppositely oriented

[1] See for example [16] for the basic definitions of Fuss–Catalan numbers, called *generalized Catalan numbers* there.
[2] All the relevant notions and terminology are reviewed in Sect. 2.5.
[3] For an explanation of the term *mind-body* see Section 2.3 of [1].

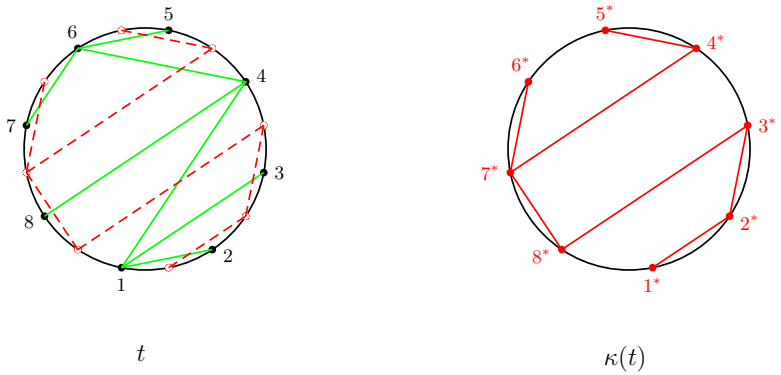

FIGURE 2. The complement defined in [15]

surface, so that we get a duality $\mathcal{N} \to \mathcal{N}^\intercal$, where $\mathcal{N}$ stands for the set of trees pegged in the standard disk with the counterclockwise orientation, and $\mathcal{N}^\intercal$ for the set of trees pegged in the disk with the clockwise orientation.

As observed in Section 5 of [1] this drawback can be rectified using mind-body duality at the level of *rooted edge-labeled* trees. The upshot is that one can define an involutory duality $*\colon \mathcal{N} \to \mathcal{N}$ lifting the duality of unlabeled trees by

$$t^* = s(\kappa(t)), \tag{1.1}$$

where $s\colon \mathcal{N} \to \mathcal{N}$ stands for the map induced by reflection of the circle across the diameter that passes through the vertex labeled 1. We emphasize that we consider reflections and rotations to act on the edges of non-crossing trees leaving the vertices fixed, so t^* is still pegged on the standard disk endowed with the counterclockwise orientation. More concretely, the nc-dual t^* of a non-crossing tree t is obtained by labeling the dual vertices in a *clockwise* order starting with the dual vertex that immediately follows the vertex of t labeled 1, and then transferring the dual tree to the counterclockwise oriented circle. For example, see Fig. 3 for the dual of the non-crossing tree of Fig. 2.

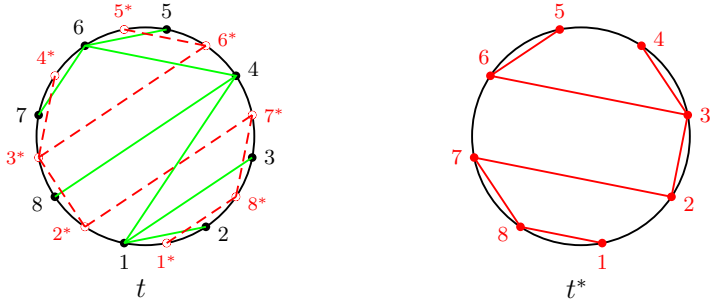

FIGURE 3. The dual of a non-crossing tree

We note that there is a price to be paid for getting the dual of a non-crossing tree to be pegged in the same oriented disk, namely the natural correspondence between the edges of two dual trees is lost. In the case of mind-body duality each edge of t crosses once only one edge of t^* and so every edge e of t has a dual edge e^* in t^* with a natural topological relation. No such topologically obvious correspondence exists between the edges of two nc-dual labeled non-crossing trees.

This duality for non-crossing trees and the necessary background material about pegs are developed in Sect. 2.5.

The set of non-crossing trees $\mathcal{N} = \bigsqcup_{m\geq 0} \mathcal{N}_m$, where $\mathcal{N}_m$ is the set of non-crossing trees with m edges is an example of a $(p = 3)$ Fuss–Catalan family. Fuss–Catalan families have been extensively studied in the literature from various points of view, see for example [4], [16], and [23]. It turns out that nc-duality is an instance of a duality that exists in all such families.

Inspired by [4] we consider $(p = 3)$ Fuss–Catalan families as instances of the *free ternary magma with one generator*, that is a set with a ternary operation satisfying the usual universal property of "freeness", we give the details in Sect. 2.1, including a standard construction of the ternary magma freely generated by a set X as a set of words. There is a natural notion of *rank* for elements of a free ternary magma M namely the number of occurrences of the ternary operator and we denote by M_m the set of elements of M that have rank m.

Among the many instances of Fuss–Catalan families (or ternary magmas freely generated by one element λ) we consider in Sect. 2

- The "standard" ternary magma freely generated by one element:

$$\mathcal{A} = \bigsqcup_{m\geq 0} \mathcal{A}_m$$

  where $\mathcal{A}_m$ is the set of elements of rank m, and is usually thought of as ways of parenthesizing m applications of a ternary operation. The basic theory of free ternary magmas is developed in Sect. 2.1.
- The set of (full) ternary trees, where a ternary tree is an ordered tree with the out-degree of every vertex 0 or 3:

$$\mathcal{T} = \bigsqcup_{m\geq 0} \mathcal{T}_m.$$

  The rank is the number of internal vertices and the generator λ is the ternary tree with one vertex and no edges. For details see Sect. 2.3.
- The set of labeled non-crossing trees

$$\mathcal{N} = \bigsqcup_{m\geq 0} \mathcal{N}_m.$$

  The rank is given by the number of edges and the generator λ is the non-crossing tree with one vertex and no edges. The ternary structure of $\mathcal{N}$ is exposed in Sect. 2.7.

- The set of flagged Perfectly Chain Decomposed Ditrees (PCDDs)

$$\mathcal{P} = \bigsqcup_{m\geq 0} \mathcal{P}_m.$$

This set arises from the application of the concept of medial digraph (developed in Section 2.2 of [1]) in our case. A *ditree* is a digraph with underlying graph a tree, and a *medial ditree* is a ditree with the in and out degrees of every vertex at most 2. A *Perfectly Chain Decomposed Ditree* (PCDD) is a medial ditree endowed with a *Perfect Chain Decomposition* (PCD), that is, a decomposition of its edges into chains with the property that each vertex belongs to exactly two chains. A *flagged Perfectly Chain Decomposed Ditree* is a PCDD with a distinguished chain called its flag. The rank of an element of $\mathcal{P}$ is the number of its vertices, and the generator is the degenerated empty PCDD. For details, see Sect. 2.6.

- The set of quadrangular dissections of polygons

$$\mathcal{Q} = \bigsqcup_{m\geq 0} \mathcal{Q}_m.$$

By a quadrangular dissection of a (convex) polygon we mean a dissection of the polygon into quadrangular cells via a set of non-crossing diagonals. It is easy to see that only polygons with an even number of vertices admit quadrangular dissections.
To understand the ternary structure it is more convenient to think of elements of $\mathcal{Q}$ as 4-clusters, that is 2-complexes obtained by gluing quadrangular cells along edges in such a way that no 1-cycles are created, see Sect. 2.4 for details. The rank is given by the number of 2-cells and the generator λ is the (trivial) 4-cluster consisting of a single edge and no 2-cells.

The number of rank m elements of a ternary magma freely generated by one element is given by the ($p = 3$) Fuss–Catalan numbers

$$\nu_m := \frac{1}{2m+1}\binom{3m}{m}. \tag{1.2}$$

There are many proofs of this result, and in Theorem 2.2 we generalize the proof in [4] to prove that the number of k-tuples of rank m is the *Raney number* $R(3, k, m)$. To our knowledge this is the only elementary (without use of generating functions) proof of that result.

Any two ternary magmas freely generated by one element are isomorphic via a unique isomorphism and we call any such isomorphism a *structural bijection*. Uniqueness implies that any diagram of structural bijections commutes

and in particular Diagram (1.3) commutes.

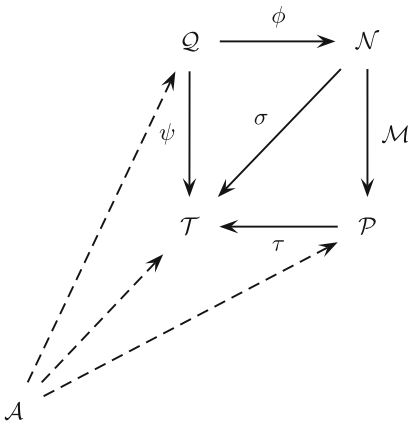

(1.3)

Interchanging the first and third argument in any occurrence of the ternary operator while leaving the second argument fixed defines a duality in $\mathcal{A}$, that satisfies, and is determined by, a fundamental equation namely Eq. (2.2). This duality is transferred via the structural bijection to a duality in any ternary magma freely generated by one element. In the magmas we consider these turn out to be quite natural and/or known:

- In $\mathcal{T}$ it transfers to interchanging the left and right subtree of every internal vertex. This duality was considered in [6].
- In $\mathcal{N}$ it transfers to nc-duality.
- In $\mathcal{P}$ it transfers to "mind-body" duality. A PCD is determined by a binary choice at every vertex: choosing which incoming edge to connect to which outgoing one. Mind-body duality consists of making the opposite choice at every vertex. See Section 2.2 of [1] for details.
- In $\mathcal{Q}$ it transfers to reflection across the perpendicular bisector of an edge.

For brevity we will refer to a ternary magma freely generated by one element and endowed with the above duality as a *free* $*$*-magma*. One of the original motivations for the present work was to understand self-duality for (labeled and unlabeled) non-crossing trees. We achieve that for the labeled case in Theorem 2.8 where we provide an explicit formula for the number of self-dual elements with given rank of a free $*$-magma. This formula was proven in [6] in the case of ternary trees using a generating function argument. We prove it by giving, in Theorem 2.7, bijections from the set of self-dual elements of rank m, to the set of elements of rank $m/2$ for m even, and to the set of pairs of elements or total rank $(m-1)/2$ for m odd. Since we have given, in Theorem 2.2, an elementary proof for the counting formulae of these sets, our proof of Theorem 2.8 is completely elementary.

The structural bijections in Diagram (1.3) have interesting combinatorial and/or topological interpretations which we explain in Sect. 3.

The interpretation of $\psi\colon\ \mathcal{Q} \to \mathcal{T}$ was given in [16]. We give an exposition of that interpretation in Sect. 3.1.

We give an interpretation of $\phi\colon\ \mathcal{Q}_m \to \mathcal{N}_m$ in Sect. 3.3. Consider a quadrangular dissection q. The dissected polygon has an even number of vertices and it is easy to see that the dissecting diagonals connect vertices with labels of opposite parities and therefore one of the diagonals of a cell of q connects vertices with odd labels while the other one vertices with even labels. The non-crossing tree $\phi(q)$ is then obtained by the "odd" diagonals of all the cells. This interpretation is, to our knowledge, new. There is however a close connection between ϕ and the Schaeffer bijection between rooted quadrangulations of the sphere and well labeled trees given in [29] (see also [3])[4]. To explain this connection, in Sect. 3.3.1, we define (in Sect. 2.5.1) the set $\mathcal{BO}_m$ of *bipartisan trees* with m edges, and exhibit a bijection $\mathcal{N}_m \to \mathcal{BO}_m$. A bipartisan tree is an ordered tree where the children of each non-root vertex are divided into two sets the *left children* and the *right children*, in such a way that all the right children are less than the left ones.

Actually ϕ preserves more structure, it is equivariant with respect to two actions of the dihedral group $\mathrm{D}_{2(m+1)}$ with $4(m+1)$ elements. The action on $\mathcal{Q}_m$ is induced by the defining action on a regular polygon, and the action on $\mathcal{N}_m$ is generated by κ and s (see the Eq. (1.1)). Furthermore the action of the subgroup generated by κ^2 and s is the standard action of D_{m+1} on $\mathcal{N}_m$. This observation allows us to achieve our goal of enumerating self-dual unlabeled non-crossing trees in Sect. 4.

A rank preserving bijection $\mathcal{N} \to \mathcal{T}$ has been given in [8] modulo an arbitrary choice when $m = 2$, and it turns out that with the appropriate choice that bijection is exactly the structural bijection, see Sect. 3.2. Since by the commutativity of Diagram (1.3), $\sigma = \psi \circ \phi^{-1}$ we have an interpretation of σ as well.

In Sect. 4, we examine the dihedral action on $\mathcal{Q}_m$ and in Theorem 4.1 we count its fixed points. This allows us to use Burnside's Lemma to deduce explicit formulae for the numbers of quadrangular dissections of a $2(m+1)$-gon up to rotations, and up to rotations and reflections. These formulae do not appear to be previously known. As a corollary we also reprove the formula for the number of unlabeled non-crossing trees in [22].

Additionally, Theorem 4.1 in combination with the "Counting Lemma" of Robinson (Lemma 4.5, see [26]) allows us to get explicit formulae for the number of unlabeled self-dual (oriented or not) non-crossing trees, one of the original motivations of this work.

We conclude with some future directions and open questions in Sect. 5.

1.1. Conventions, Notation, Terminology

Throughout the paper we use standard notation and terminology, with a few exceptions that we explain now.

We use the notation $[n] := \{1, \ldots, n\}$. For a finite set X we denote its *cardinality* by $|X|$. For a set X, a subset of X with k elements (respectively,

[4] Thanks to the anonymous referee of a previous version for pointing this out.

an ordered k-tuple of distinct elements of X) is called a *k-combination* (respectively, *a k-permutation*) of elements of X.

For a graph its *order* is the number of its vertices, and its *size* is the number of its edges. We typically denote by n the order of a graph and by m its size, and since we are typically dealing with trees, very often we have $n = m + 1$. We call the set of all edges incident to a given vertex v the *star* of v.

We also use the abbreviations, v-graph (respectively e-graph) for a graph with vertices (respectively, edges) labeled by the elements of $[n]$ (respectively $[m]$). An e-v-graph is a graph with vertices labeled by $[n]$ and edges labeled by $[m]$.

A *ditree* is a directed tree, that is, a digraph with underlying undirected graph a tree. A *dag* is a *Directed Acyclic Graph*, that is a digraph with no *oriented* cycles. A *topological sort* of a dag is a linear order of its vertices that extends the corresponding partial order.

Our rooted trees grow upwards and, consistently with the standard orientation of the plane, the children of a vertex of an ordered tree increase from right to left.

Rotations of the disk are assumed to be counterclockwise unless explicitly specified otherwise.

For a set X, we denote the symmetric group of X by S_X and when $X = [n]$ we just use the symbol S_n. We multiply permutations from left to right so that $(1\,2)(1\,3) = (1\,2\,3)$.

Finally, we use left and right exponential notation for conjugation in a group, i.e. $g^h := h^{-1}gh$ and ${}^h g := hgh^{-1}$.

2. Ternary Magmas

2.1. Basic Theory

By a *ternary magma* we mean a set M endowed with a ternary operation $\Upsilon\colon\ M^3 \to M$, which we call *fusion*. As expected, a homomorphism of ternary magmas is a map that preserves the ternary operation and a homomorphism that has an inverse is called an isomorphism.

If M is a ternary magma and $X \subset M$ we say that M is *freely generated* by X if for every ternary magma N and any function $f\colon\ X \to N$, there exists a *unique* ternary homomorphism $\phi\colon\ M \to N$ extending f, i.e. so that the following diagram commutes:

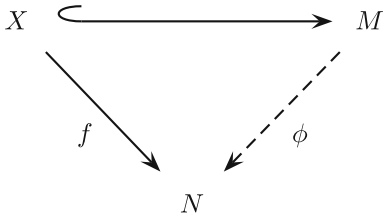

where the top arrow stands for the inclusion of X into M.

Let $X = \{\lambda_1, \ldots, \lambda_n\}$ be a set with n elements. One particular realization of the ternary magma freely generated by X is as the set of words $M(X)$ on the alphabet $\{\lambda_1, \ldots, \lambda_n, \Upsilon, (,)\}$ defined recursively by the rules:

- $\lambda_i \in M(X)$, for $i = 1, \ldots, n$,
- if $w_\mathrm{l}, w_\mathrm{m}, w_\mathrm{r} \in M(X)$ then $\Upsilon(w_\mathrm{l}, w_\mathrm{m}, w_\mathrm{r}) \in M(X)$,

with the tautological ternary operator $(w_\mathrm{l}, w_\mathrm{m}, w_\mathrm{r}) \mapsto \Upsilon(w_\mathrm{l}, w_\mathrm{m}, w_\mathrm{r})$.

Clearly for any element $x \in M(X)$ that is not a generator there are *uniquely determined* elements x_l, x_m, and x_r such that $x = \Upsilon(x_\mathrm{l}, x_\mathrm{m}, x_\mathrm{r})$.

Definition 2.1. The *rank*, $\mathrm{rk}(w)$, of an element $w \in M(X)$ is the number of occurrences of the letter "Υ" (or equivalently the number of matching pairs of parentheses "$(,)$") in w. For a free ternary magma M we will denote the set of elements of rank m by M_m.

More generally, for a free ternary magma, we define the rank of an element $\bar{a} = (a_1, \ldots, a_k) \in M^k$ as the sum of the ranks of its coordinates, i.e.

$$\mathrm{rk}(\bar{a}) = \mathrm{rk}(a_1) + \cdots + \mathrm{rk}(a_k)$$

and we denote the set of elements of M^k of rank m by $\left(M^k\right)_m$. The rank of a k-combination of elements of M is defined similarly.

An easy inductive argument shows that an element of $\left(M^k\right)_m$ has $2m+k$ occurrences of λ_is.

By standard abstract nonsense we have that any bijection between X and Y extends to an isomorphism between $M(X)$ and $M(Y)$, and so, up to isomorphism, it makes sense to talk about the free ternary magma with n generators. When the generators are not important we will just use $M(n)$ to denote the free ternary magma with n generators.

Our main interest is in the special case that the generating set contains only one element λ. In that case for any ternary magma N the choice of one element $n_0 \in N$ determines a unique homomorphism $f\colon M \to N$ with $f(\lambda) = n_0$. In particular any two ternary magmas freely generated by a single element are isomorphic via a *unique* isomorphism. So it makes sense to talk about *the* ternary magma freely generated by one element. We will denote the ternary magma freely generated by one element by $\mathcal{A}$, so that we have the following recursive definition:

$$\mathcal{A} = \bigcup_{m \geq 0} \mathcal{A}_m$$

where

- $\mathcal{A}_0 = \{\lambda\}$,
- $\mathcal{A}_{m+1} = \{\Upsilon(a_\mathrm{l}, a_\mathrm{m}, a_\mathrm{r}) : a_\mathrm{l} \in \mathcal{A}_i, a_\mathrm{m} \in \mathcal{A}_j, a_\mathrm{r} \in \mathcal{A}_k, \quad i + j + k = m\}$.

We will refer to the unique isomorphism between two ternary magmas freely generated by one element as the *structural bijection*.

It is well known that $\mathcal{A}_m$ is counted by the ($p = 3$) Fuss–Catalan numbers

$$|\mathcal{A}_m| = \nu_m := \frac{1}{2m+1}\binom{3m}{m}. \tag{2.1}$$

We present a proof of Eq. (2.1) next. In fact, using a slight generalization of the method of [4], we prove the following more general theorem.

Theorem 2.2. *The number of rank m elements of $\mathcal{A}^k$ is given by*

$$\left|\left(\mathcal{A}^k\right)_m\right| = \frac{k}{2m+k}\binom{3m+k-1}{m}.$$

Definition 2.3. An element of $M(n)^k$, or a combination of elements of $M(n)$, is called *repetition-free* if no generator repeats, that is the arguments of all occurrences of Υ are pairwise distinct.

Notice that there are repetition-free elements of rank m in $M(n)^k$ if and only if $n \geq 2m+k$.

Lemma 2.4. *The number of repetition-free k-combinations of elements of $M(2m+k)$ of rank m is*

$$\frac{(3m+k-1)!}{m!(k-1)!}.$$

Proof. Let C be the set of such combinations. We will construct a bijection $f\colon C \to W$, where W is the set of m-combinations of words of length 3 from the alphabet $[3m+k-1]$ with the property that all the symbols that occur are distinct. In other words an element of W is a set $\{a_{11}\,a_{12}\,a_{13}, \ldots, a_{m1}\,a_{m2}\,a_{m3}\}$ obtained by splitting a $3m$-permutation of $[3m+k-1]$ into m words of length 3. Such a set of words is obtained by first choosing $k-1$ symbols to be omitted from $[3m+k-1]$, and then a permutation of the remaining $3m$ symbols. Since the order of the words is not important, every element of W is obtained by $m!$ such choices. So:

$$\begin{aligned}|W| &= \binom{3m+k-1}{k-1}\frac{(3m)!}{m!}\\ &= \frac{(3m+k-1)!}{m!(k-1)!}.\end{aligned}$$

Let $\bar{p} = \{p_1, \ldots, p_k\}$ be an element of C. Call an occurrence of Υ in $\bar{p}$ *innermost* if all three arguments are λ_is.

In what follows, we will just use i to stand for λ_i.

To find $f(\bar{p})$, the word that corresponds to $\bar{p}$, we start by ordering all innermost occurrences of Υ with respect to increasing largest argument and call the smaller such innermost occurrence $2m+k+1$. One of our 3-letter words will be formed by the three arguments of that occurrence. Replacing that occurrence with $2m+k+1$ gives us a k-combination of elements of a ternary magma freely generated by $2(m-1)+k$ elements.

Proceeding inductively we replace the smallest inner occurrence of Υ in this combination with $2m+k+2$ and let its arguments form our second word, and so on until we obtain a set of m words each of length 3.

Conversely, let $w = \{w_1, w_2, \ldots, w_m\}$ be an element of W. To find $f^{-1}(w)$, we order the words with respect to increasing largest element and call them $2m+k+1, \ldots, 3m+k$ in that order.

Notice that all the symbols that occur in the word named $2m+k+i$ are less than $2m+k+i$, for $i=1,\ldots,m$. Indeed, for each i there are $m-i$ words larger than $2m+k+i$, and so there need to be at least $m-i$ elements of $[3m+k-1]$ larger than the largest element of that word that have not been used before.

Let $r_1,\ldots,r_{k-1},3m+k$ be the k symbols from $[3m+k]$ that do not occur in any of the w_is. If $r_i > 2m+k$, i.e. it is not a generator of $M(2k+2)$, replace the corresponding word, say $x_{\mathrm{l}}\, x_{\mathrm{m}}\, x_{\mathrm{r}}$ with $\Upsilon\left(x_{\mathrm{l}}, x_{\mathrm{m}}, x_{\mathrm{r}}\right)$. Proceed recursively to get a set of k elements of total rank m. □

We give two examples to illustrate the proof. As in the body of the proof we use i to stand for λ_i.

Example 1. Consider $m=6$ and the following triple of elements of $M(15)$:

$$3,\quad \Upsilon\left(4,\Upsilon\left(6,8,5\right),9\right),\quad \Upsilon\left(\Upsilon\left(12,2,7\right),13,\Upsilon\left(10,\Upsilon\left(11,15,1\right),14\right)\right).$$

Inductively, we get the sequence:

$$\begin{aligned}16&=6\,8\,5\\17&=12\,2\,7\\18&=11\,15\,1\\19&=4\,16\,9\\20&=10\,18\,14\\21&=17\,13\,20\end{aligned}$$

Thus this triple corresponds to the following set of words:

$$\{6\,8\,5, 12\,2\,7, 11\,15\,1, 4\,16\,9, 10\,18\,14, 17\,13\,20\}.$$

Example 2. Conversely, for $m=6$ and $k=3$ let us take the set of words from Example 1:

$$\{6\,8\,5, 12\,2\,7, 11\,15\,1, 4\,16\,9, 10\,18\,14, 17\,13\,20\}.$$

To find the corresponding pair of elements we start by observing that the omitted symbols are $3, 19, 21$. Label the words as:

$$\begin{aligned}16&=6\,8\,5\\17&=12\,2\,7\\18&=11\,15\,1\\19&=4\,16\,9\\20&=10\,18\,14\\21&=17\,13\,20\end{aligned}$$

and expanding successively we get the triple:

$$\begin{aligned}T&=3,\quad 19,\quad 21\\&=3,\quad \Upsilon\left(4,16,9\right),\quad \Upsilon\left(17,13,20\right)\\&=3,\quad \Upsilon\left(4,\Upsilon\left(6,8,5\right),9\right),\quad \Upsilon\left(\Upsilon\left(12,2,7\right),13,\Upsilon\left(10,18,14\right)\right)\\&=3,\quad \Upsilon\left(4,\Upsilon\left(6,8,5\right),9\right),\quad \Upsilon\left(\Upsilon\left(12,2,7\right),13,\Upsilon\left(10,\Upsilon\left(11,15,1\right),14\right)\right).\end{aligned}$$

Now we can prove Theorem 2.2.

Proof of Theorem 2.2. By Lemma 2.4 we have that the number of k-tuples of repetition-free elements of $M(2m+k)$ of rank m is

$$k!\frac{(3m+k-1)!}{m!(k-1)!} = k\frac{(3m+k-1)!}{m!}.$$

Now there is a $(2m+k)! : 1$ map from the set of such tuples to $\left(\mathcal{A}^k\right)_m$ given by replacing all generators λ_i by the single generator λ. It follows that

$$\begin{aligned}\left|\left(\mathcal{A}^k\right)_m\right| &= \frac{k}{(2m+k)!}\frac{(3m+k-1)!}{m!} \\ &= \frac{k}{2m+k}\binom{3m+k-1}{m}.\end{aligned}$$

□

Remark 2.5. The proof of Theorem 2.2 given above for $k=1$ appears in [4] in the more general context of p-ary magmas. We chose to expose only the case $p=3$, but the proof, *mutatis mutandis*, easily works in the general case. One gets that the number of k-tuples of rank m of elements of the p-ary magma freely generated by one element is given by the *Raney number* $R(p,k,m)$, that is,

$$R(p,k,m) = \frac{k}{(p-1)m+k}\binom{pm+k-1}{m}.$$

An equivalent formula appears in page 201 of [12], see also [17]. As far as we know the above is the only elementary (without the use of generating functions) proof of this result.

2.2. Duality in $\mathcal{A}$

There is a natural duality in $\mathcal{A}$ defined by recursively interchanging the left and right argument of any instance of Υ while leaving the middle argument fixed[5]. Formally, the duality is recursively defined by

$$\begin{aligned}\lambda^* &= \lambda \\ \Upsilon\left(a_{\mathrm{l}}, a_{\mathrm{m}}, a_{\mathrm{r}}\right)^* &= \Upsilon\left(a_{\mathrm{r}}^*, a_{\mathrm{m}}^*, a_{\mathrm{l}}^*\right)\end{aligned} \tag{2.2}$$

and it is clearly rank preserving.

This duality is transferred via the structural bijection to a duality in any free ternary magma with one generator. In what follows we will refer to a free ternary magma with one generator endowed with that duality as a *free $*$-magma*. In the following subsections we will see that many well known dualities are simply manifestations of the fact that the underlying set is a free $*$-magma.

Definition 2.6. An element of $\mathcal{A}$ is called *self-dual* if $a^* = a$. We let $\mathcal{S} := \{a \in \mathcal{A} : a^* = a\}$ and we denote by $\mathcal{S}_m$ the set of rank m elements of $\mathcal{S}$.

[5]This definition was given for ternary trees in [6]. See also Remark 2.9.

Theorem 2.7. *For even m, $\mathcal{S}_m$ is in bijection with $\mathcal{A}_{\frac{m}{2}}$, while for m odd $\mathcal{S}_m$ is in bijection with $\left(\mathcal{A}^2\right)_{\frac{m-1}{2}}$.*

Proof. By Eq. (2.2), we have that if $a \in \mathcal{S}$ then

1. $a_{\mathrm{r}} = a_{\mathrm{l}}^*$,
2. $a_{\mathsf{m}} \in \mathcal{S}$, and therefore
3. $\mathrm{rk}(a) = 2\mathrm{rk}(a_{\mathrm{l}}) + \mathrm{rk}(a_{\mathrm{m}}) + 1$.

For each m we will recursively define a bijection β_m that sends a self-dual element a of rank m to an element of $\mathcal{A}_{\frac{m}{2}}$ when m is even and an element of $\left(\mathcal{A}^2\right)_{\frac{m-1}{2}}$ when m is odd. For $m = 0, 1$ all relevant sets have one element so β_m is defined. Assume then that such a bijection β_k has been defined for all values $k < m$ and let $a \in \mathrm{S}_m$.

If m is even the third item above implies that a_{m} is a self dual element of odd rank, so $\beta_{\mathrm{rk}(a_{\mathrm{m}})}$ is a pair of elements of $\mathcal{A}$. We can then define $\beta_m(a) = \Upsilon\left(a_{\mathrm{l}}, \beta_{\mathrm{rk}(a_{\mathrm{m}})}(a_{\mathrm{m}})\right)$.

If m is odd then a_{m} has even rank and $\beta_{\mathrm{rk}(a_{\mathrm{m}})}(a_{\mathrm{m}})$ is an element of $\mathcal{A}_{\frac{\mathrm{rk}(a_{\mathrm{m}})}{2}}$. We can then define $\beta_m(a) = (a_{\mathrm{l}}, \beta_{\mathrm{rk}(a_{\mathrm{m}})}(a_{\mathrm{m}}))$.

To simplify notation we use β without subscripts. To see that β is indeed a bijection notice that if $b \in \mathcal{A}_k$ then $\beta^{-1}(b) = \Upsilon\left(b_{\mathrm{l}}, \beta^{-1}(b_{\mathrm{m}}, b_{\mathrm{r}}), b_{\mathrm{l}}^*\right)$, while if $(a, b) \in \left(\mathcal{A}^2\right)_k$ then $\beta^{-1}(a, b) = \Upsilon\left(a, \beta^{-1}(b), a^*\right)$. □

So as a corollary, using the cases $k = 1$ and $k = 2$ of Theorem 2.2 we have the following explicit formula for s_m the number of self-dual elements of $\mathcal{A}$ of rank m.

Theorem 2.8. *The number of self-dual elements of $\mathcal{A}_m$ is*

$$s_m = \begin{cases} \dfrac{1}{2k+1}\dbinom{3k}{k} & \text{if } m = 2k \\ \dfrac{1}{k+1}\dbinom{3k+1}{k} & \text{if } m = 2k+1. \end{cases}$$

Remark 2.9. Equation (2.2) was used in [6] to deduce the formula of Theorem 2.8 using a generating function argument. In that paper the authors prove that s_m is the number of self-dual ternary trees[6] with m internal vertices.

Remark 2.10. If M is any ternary magma then $\mathcal{A}_m$ acts on M^{2m+1} in an "operadic way". Namely consider an element $a \in \mathcal{A}_m$ and $\bar{x} \in M^{2m+1}$, and think of the occurrences of λ in a as placeholders, the action $a \cdot \bar{x}$ is then given by substituting x_i, the ith coordinate of $\bar{x}$ for the ith occurrence of λ and evaluating the resulting expression in M. The basic property of this "action" is the following operadic property: let $a = \Upsilon\left(a_{\mathrm{l}}, a_{\mathrm{m}}, a_{\mathrm{r}}\right)$ with $\mathrm{rk}(a_{\mathrm{l}}) = m_1$, $\mathrm{rk}(a_{\mathrm{m}}) = m_2$, and $\mathrm{rk}(a_{\mathrm{r}}) = m_3$, and let $\bar{x} \in M^{2m+1}$. Write $\bar{x}$ as the concatenation of $\bar{x}_{\mathrm{l}}$, $\bar{x}_{\mathrm{m}}$, and $\bar{x}_{\mathrm{r}}$, where $\bar{x}_{\mathrm{l}} \in M^{2m_1+1}$, $\bar{x}_{\mathrm{m}} \in M^{2m_2+1}$, and $\bar{x}_{\mathrm{r}} \in M^{2m_3+1}$. Then we have

$$\Upsilon\left(a_{\mathrm{l}}, a_{\mathrm{m}}, a_{\mathrm{r}}\right) \cdot (\bar{x}_{\mathrm{l}}, \bar{x}_{\mathrm{m}}, \bar{x}_{\mathrm{r}}) = \Upsilon(a_{\mathrm{l}} \cdot \bar{x}_{\mathrm{l}}, a_{\mathrm{m}} \cdot \bar{x}_{\mathrm{m}}, a_{\mathrm{r}} \cdot \bar{x}_{\mathrm{r}}).$$

[6] Called "symmetric ternary trees" there.

This interpretation of $\mathcal{A}$ as operators is well known to computer scientists especially with the realization of $\mathcal{A}$ as the set of ternary trees.

Remark 2.11. The motivation of this work was to understand duality of nc-trees and so the focus has been in ternary operations. However, the results of this section can be carried over, almost verbatim, to p-ary operations for any natural number p, see also Remark 2.5.

The free p-magma with one generator $\mathcal{A}_p$ (defined in a manner entirely analogous to the ternary case) admits a duality given by permuting the arguments of every occurrence of the p-ary operation via the involution $i \mapsto p+1-1$. Letting $\mathcal{A}^k_{p;m}$ (respectively $\mathcal{S}_{p;m}$) stand for the set of k-tuples of elements of $\mathcal{A}_p$ (respectively self-dual elements of $\mathcal{A}_p$) of rank m, we have the following result generalizing Theorem 2.7.

Theorem 2.12. *If $p = 2k$ is even then*

- *The generator λ is a self-dual element of rank 0. There are no other self-dual elements of even rank.*
- *$\mathcal{S}_{p;m}$ is in bijection with $\mathcal{A}^k_{p;\frac{m-1}{2}}$ for m odd.*

If $p = 2k-1$ is odd then

- *$\mathcal{S}_{p;m}$ is in bijection with $\mathcal{A}_{p;\frac{m}{2}}$ for m even.*
- *$\mathcal{S}_{p;m}$ is in bijection with $\mathcal{A}^k_{p;\frac{m-1}{2}}$ for m odd.*

2.3. Ternary Trees

Perhaps the most well-known example of a free $*$-magma is the set of (full) ternary trees $\mathcal{T}$. A ternary tree is an ordered tree where every internal vertex has exactly three children. The standard recursive definition of ternary trees[7] exhibits $\mathcal{T}$ as a ternary magma freely generated by λ, the ternary tree consisting of a single vertex, the root, and no edges. If t_l, t_m, and t_r are three ternary trees, then their fusion $\Upsilon(t_\mathrm{l}, t_\mathrm{m}, t_\mathrm{r})$ is defined by adding a new vertex v_0 declaring it to be the root, and adding edges from v_0 to the roots of t_l, t_m, and t_r, see Fig. 4 for an example.

The leaves of a ternary tree, from left to right correspond to occurrences of λ while the internal vertices to occurrences of Υ, so that $\mathcal{T}_m$ consists of all ternary trees with m internal vertices and therefore, $2m+1$ leaves. An innermost occurrence of Υ (see the proof of Lemma 2.4) corresponds to *extremal inner vertices*, that is inner vertices with only leaves as children. The action of $\mathcal{A}$ on a ternary magma M described in Remark 2.10 has the following graphical interpretation: Let $\bar{x} = (x_1, \ldots, x_{2m+1}) \in M^{2m+1}$ and $t \in \mathcal{T}_m$ corresponding to $a \in \mathcal{A}_m$ under the structural bijection. To find $a \cdot \bar{x}$ label the leaves of t with the coordinates of $\bar{x}$ as you encounter them from left to right. Label every extremal internal vertex with children labeled x_l, x_m, x_r by $\Upsilon(x_\mathrm{l}, x_\mathrm{m}, x_\mathrm{r})$, and proceed to label each vertex that has all its children labeled by the fusion of its children. Then $a \cdot \bar{x}$ is the label of the root.

[7] See for example [27, sections 5.3 and 11.1], or any "Discrete Mathematics" textbook.

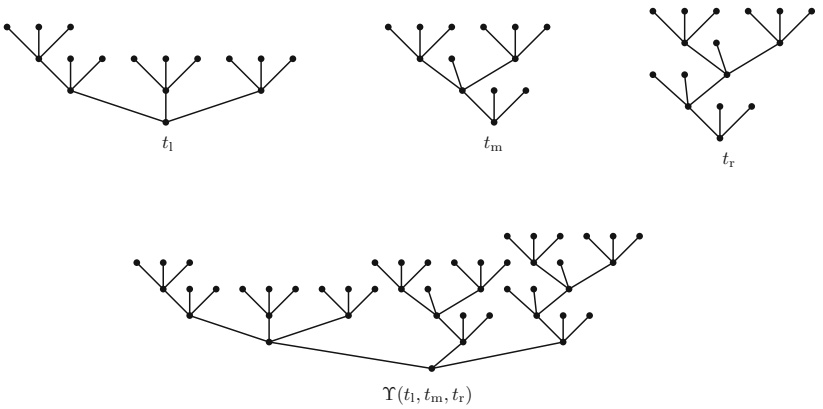

FIGURE 4. Fusion of ternary trees

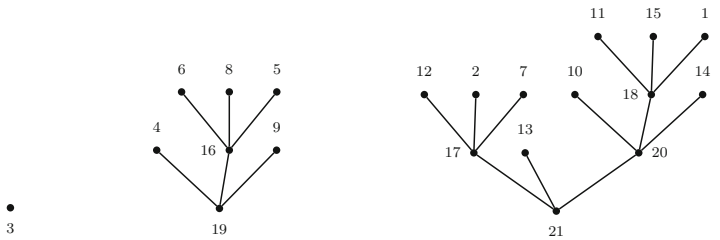

FIGURE 5. The forest of ternary trees corresponding to Examples 1 and 2

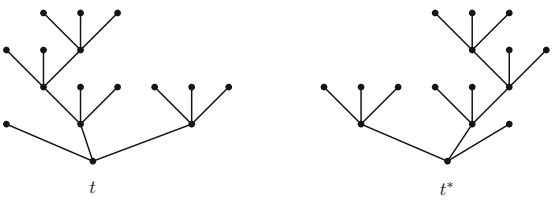

FIGURE 6. A ternary tree and its dual

The proof of Lemma 2.4 admits also a graphical interpretation that we leave to the so inclined reader. The triple of elements in Examples 1 and 2 corresponds to the forest of three ternary trees in Fig. 5.

For a ternary tree t its dual t^* is obtained by interchanging the left and right subtrees of every internal vertex. "Geometrically" the duality $*$ can be interpreted as "reflection" across the middle for all subtrees, see Fig. 6 for an example.

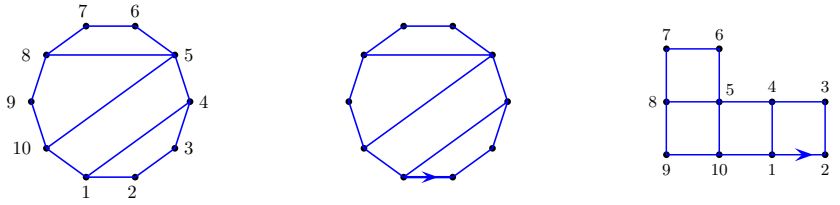

FIGURE 7. A quadrangular dissection of a decagon and the associated 4-cluster

2.4. Quadrangular Dissections of a Polygon

By a *quadrangular dissection* q of a vertex-labeled polygon P we mean a subdivision of P into quadrangular cells by means of non-intersecting diagonals. An example of a quadrangular dissection of a decagon is shown on the left side of Fig. 7, the middle of the same figure shows the same dissection with the labels of the polygon suppressed, instead we have chosen a *root edge* which stands for the edge 1 2; clearly the labels of the polygon can be deduced from the root edge and the standard (counterclockwise) orientation of the plane. In what follows we will routinely identify quadrangular dissections of a labeled polygon with rooted dissections of an unlabeled polygon, and refer to the cell containing the root edge as the *root cell*, and to the starting vertex of the root edge as the *root vertex*.

Let $\mathcal{Q} = \bigcup_{m\geq 0} \mathcal{Q}_m$, where $\mathcal{Q}_m$ denotes the set of quadrangular dissections with m cells. In the spirit of [14], we can consider quadrangular dissections as 4-clusters, that is as 2-complexes defined recursively as follows: the only element of $\mathcal{Q}_1$ is the standard square with root edge the bottom one oriented from left to right. If $q \in \mathcal{Q}_m$ is a 4-cluster with m cells, then the 2-complex obtained by gluing a new square p to q by identifying, via an orientation reversing homeomorphism, the root edge of p with a non-root boundary edge of q, is a 4-cluster with $m+1$ cells and root edge the root of q. The right side of Fig. 7 shows the quadrangular dissection in the left side as a 4-cluster.

We can easily check, for example using the fact that the Euler characteristic of the disk is 1, that a 4-cluster with m cells has $2m+2$ vertices and $3m+1$ edges, $m-1$ of which are diagonals of the polygon.

Remark 2.13. We emphasize that despite the term "4-cluster" and the somewhat similar pictures (see e.g. [21]) there is no direct connection with the subject of cluster algebras.

To exhibit $\mathcal{Q}$ as a free $*$-magma we define λ to be the degenerate quadrangular dissection with 0 cells consisting of a single root edge 1 2, and set $\mathcal{Q}_0 = \{\lambda\}$. For $q_{\rm l}, q_{\rm m}, q_{\rm r} \in \mathcal{Q}$, $\Upsilon(q_{\rm l}, q_{\rm m}, q_{\rm r})$ is the quadrangular dissection obtained by identifying the root edge of $q_{\rm l}$ ($q_{\rm m}$ or $q_{\rm r}$, respectively) to the left (middle or right, respectively) edge of the standard square by an orientation reversing homeomorphism, in particular $\Upsilon(\lambda,\lambda,\lambda)$ is the standard square. Clearly every quadrangulation is $\Upsilon(q_{\rm l}, q_{\rm m}, q_{\rm r})$ for some uniquely defined $q_{\rm l}$, $q_{\rm m}$,

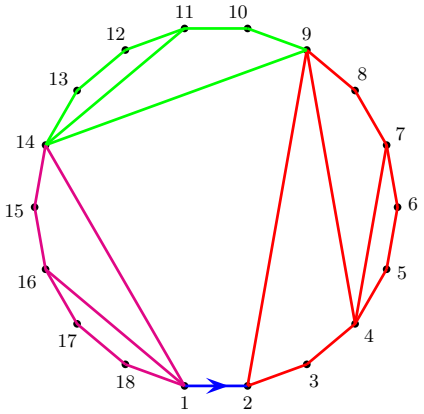

FIGURE 8. Expressing a quadrangular dissection as $\Upsilon\,(q_{\mathrm{l}}, q_{\mathrm{m}}, q_{\mathrm{r}})$

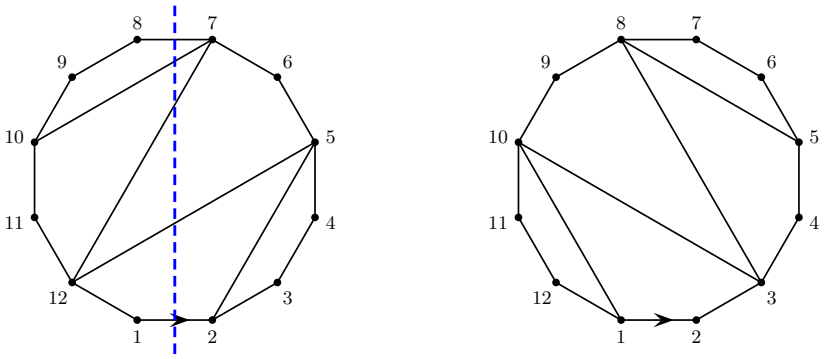

FIGURE 9. A quadrangular dissection of a dodecagon and its dual

and q_{r}. Indeed if $2\,k$ is the leftmost edge of the root cell of q and $1\,l$ the rightmost, then q_{l} (q_{m} or q_{r}, respectively) is the 4-subcluster of q spanned by the vertices $l, \ldots, 1$ ($k, \ldots, l$ or $2, \ldots, k$, respectively), see Fig. 8. Therefore, $\mathcal{Q}$ is a ternary magma freely generated by λ.

From the description of the fusion of quadrangular dissections it is clear that for $q \in \mathcal{Q}$ its dual q^* is obtained by reflecting across the perpendicular bisector of the root edge $1\,2$; see Fig. 9 for an example.

2.5. Non-crossing Trees as Properly Embedded Graphs

A non-crossing tree is a tree properly embedded (*pegged*) in a disk. The concept of graphs properly embedded in an oriented surface with boundary, and their duality, was developed in [1]. We review the basic definitions with an eye to the application of the general theory to the case of trees, so that all our examples will in fact be related to non-crossing trees. Most of the concepts are

analogous to concepts in the standard theory of cellularly embedded graphs in closed surfaces, the reader may consult [1] for details.

A *Properly Embedded Graph* (*peg* for short) is a graph embedded in a compact oriented surface with boundary in such a way that:

- the vertices of the graph lie on the boundary of the surface and the interior of the edges in the interior of the surface,
- removing the graph breaks the surface into simply connected *regions* and its boundary into *arcs*,
- each region contains exactly one arc in its boundary.

We will refer to a proper embedding as *pegging*, and the graph will be said to be *pegged* into the surface. For example in Fig. 1 we see a tree (in green) pegged into a disk.

We are really interested in pegs up to homeomorphisms of the surface and we will abuse the language and use peg to refer to an equivalence class of properly embedded graphs where two pegs are equivalent if they differ by a homeomorphism. By an *oriented peg* we mean an equivalence class of properly embedded graphs where two pegs are equivalent when they differ by an *orientation preserving* homeomorphism of the surface. When we want to emphasize that whether the homeomorphism is orientation preserving or not is irrelevant we will talk about *unoriented pegs*.

A *labeled* peg is a peg with vertices labeled by $[n]$, where n is the order of the graph and homeomorphisms between labeled pegs are required to preserve labels.

Remark 2.14. It is a consequence of the definition that if a graph is pegged in a surface then the surface homotopically retracts to the graph, and in particular its Euler characteristic is equal to the Euler characteristic of the graph. Since the disk is the only oriented surface with Euler characteristic 1 it follows that a graph pegged in a disk is a tree, and if a tree is pegged in a surface then the surface is a disk.

Definition 2.15. A *non-crossing tree* (*nc-tree* for short) is a labeled tree pegged in an disk. For concreteness (unless specified otherwise) we assume that all nc-trees are pegged in the *standard disk* i.e. the unit disk in $\mathbb{C}$, their vertices form a regular polygon, and their labels are increasing in the counterclockwise direction. We denote the set of nc-trees with m edges by $\mathcal{N}_m$, and let $\mathcal{N} = \bigcup_{m\geq 0}\mathcal{N}_m$.

An *unlabeled nc-tree* is an unlabeled tree pegged in a disk and we denote by $\widetilde{\mathcal{N}}_m$ the set of unlabeled nc-trees with m edges and let $\widetilde{\mathcal{N}} = \bigcup_{m\geq 0}\widetilde{\mathcal{N}}_m$.

An *oriented nc-tree* is an (unlabeled) oriented peg whose underlying graph is a tree, we denote by $\mathcal{N}'_m$ the set of oriented nc-trees with m edges and let $\mathcal{N}' = \bigcup_{m\geq 0}\mathcal{N}'_m$.

Remark 2.16. The symmetry group of the regular n-gon is $\mathrm{D}_n = \langle s, c\rangle$, the dihedral group with $2n$ elements, where s stands for the reflection across the diameter of the circumscribed circle of the polygon that passes through the vertex 1, and c is counterclockwise rotation by $2\pi/n$ radians. If $n = m + 1$

then D_n acts on $\mathcal{N}_m$, by rotating and reflecting the edges: for $g \in \mathrm{D}_n$, $g(t)$ has an edge $(g(i), g(j))$ if and only if t has an edge (i, j). Then $\widetilde{\mathcal{N}}_m$ is the set of orbits of this action,while $\mathcal{N}'_m$ is the set of orbits of the action of the cyclic subgroup $\langle c \rangle$.

In what follows, we will occasionally use the notation $\bar{t}$ to stand for $s(t)$.

Given a peg Γ, the orientation of the surface induces a cyclic order on the set of vertices that lie on a given connected component of the boundary, and this determines an element of $\mu(\Gamma) \in \mathrm{S}_V$ called the *monodromy* of the peg. Of course, if Γ is a labeled peg of order n, then $\mu(\Gamma)$ can be considered an element of S_n. Since the disk has only one boundary component, for an nc-tree t we have that $\mu(t)$ is an n-cycle ζ, and our convention for the labels means that $\zeta = (1\,2\,\ldots\,n)$.

The *mind-body dual peg* of a graph Γ pegged in a surface F is the peg Γ^* pegged in $F^{\intercal}$, that is, F endowed with the opposite orientation, and defined as follows:

- The vertices of Γ^* are in one-to-one correspondence with the regions of Γ; when we draw Γ^* we place its vertices on the arcs of the corresponding regions.
- The edges of Γ^* are in one-to-one correspondence with the edges of Γ, the edge e^* that corresponds to the edge e connects the vertices of Γ^* that correspond to the two regions of Γ that e lies in the boundary of.

Clearly $(\Gamma^*)^* = \Gamma$. An example of the mind-body dual for an unlabeled nc-tree is shown in Fig. 1.

There is a natural correspondence $e \mapsto e^*$ between the edges of Γ and Γ^* but no such natural correspondence exists between their vertices, so to define the dual of a labeled peg as a labeled peg we have to chose a correspondence $v \mapsto v^*$ between the vertices of Γ and those of Γ^*. There are two canonical such choices: each vertex of Γ lies in the boundary of two arcs[8], one preceding it and one following it in the cyclic order induced by the orientation, and each of these arcs contains exactly one vertex of Γ^*. Our definition of Γ^* is obtained by making the first choice, that is v^* is the vertex of Γ^* that lies in the arc following v. When need arises we will denote the dual obtained by making the second choice by $\Gamma^{\bar{*}}$. See Fig. 10 for an example, for one labeling of the unlabeled nc-tree t of Fig. 1. We emphasize that the nc-trees on the right hand side are pegged in the disk with the *opposite* (clockwise) orientation; in particular their labelings do not follow the conventions of Definition 2.15 since their vertices are decreasing if we go around the boundary circle according to the orientation. This fact is essential to ensuring that $(t^*)^* = t$ and $(t^{\bar{*}})^{\bar{*}} = t$.

A peg defines two dual structures on its underlying graph: a *Local Edge Order* (*leo* for short) and a *Perfect Trail Double Cover* (*PTDC* for short), that are analogous to a rotation scheme and a Cycle Double Cover for cellularly

[8]For general pegs these two arcs could be the same, but this cannot happen for nc-trees, except in the degenerate case of the tree with no edges.

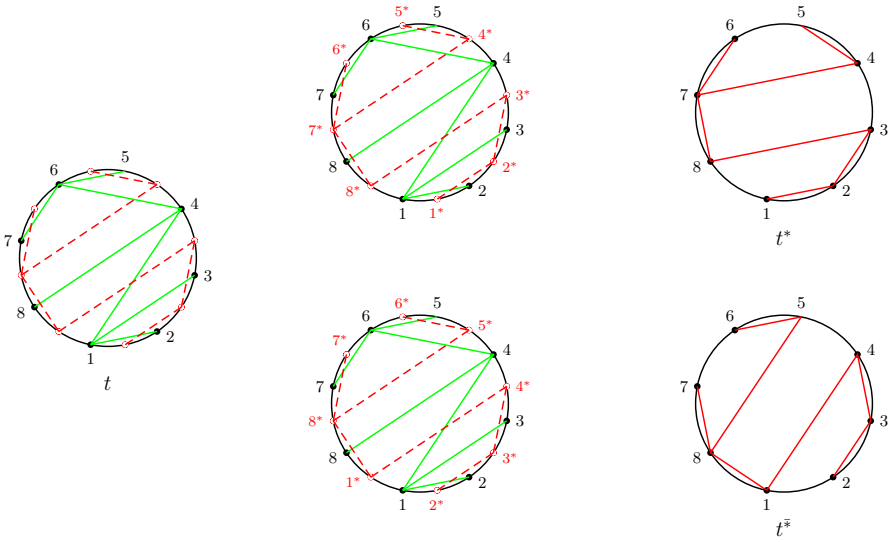

FIGURE 10. The two mind-body duals of a labeled tree pegged in a disk

embedded graphs, respectively (see [13] or [18] for basic facts and definitions for cellularly embedded graphs).

A leo is simply an assignment of a linear order to the star of each vertex of Γ, while a PTDC is a collection of positive length trails $\mathcal{T}$ such that

- each edge of Γ belongs to exactly two trails of $\mathcal{T}$,
- each vertex is the endpoint of exactly two trails of $\mathcal{T}$, and we can orient the trails of $\mathcal{T}$ in such a way that each *oriented* edge of Γ belongs to exactly one trail,
- each vertex v is the beginning of exactly one trail $\overrightarrow{v}$ and the end of exactly one trail $\overleftarrow{v}$.
- Finally, we require that unless v is a leaf the first edge of $\overrightarrow{v}$ is different than the last edge of $\overleftarrow{v}$.

Given a peg its leo is determined by the orientation of the surface: for every vertex v start slightly ahead of v in the boundary of the surface and then traverse a positively oriented loop around the vertex in the interior of the surface and order the edges incident to v in the order you encounter them. The PTDC is the collection of paths that lead from a vertex v to the next: since each region contains exactly one arc in its boundary there is a path in Γ that leads from v to the next vertex, and we define $\overrightarrow{v}$ to be that path.

The two structures are dual in the following sense: both a leo and a PTDC can be thought of as an assignment of a list of edges to each vertex. Indeed, the ordering of the star of each vertex can be given by listing the edges in order, while the trail starting at each vertex can be described as a list of edges. Mind-body duality transforms the lists coming from the leo of Γ to the

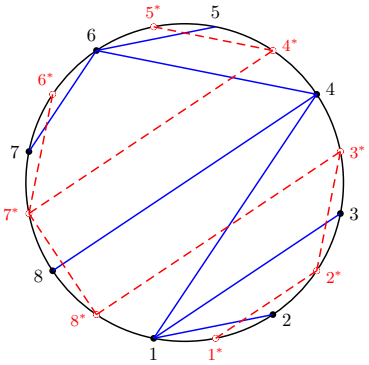

The LEO:

$1:\ 12, 13, 14$
$2:\ 21$
$3:\ 31$
$4:\ 46, 48, 41$
$5:\ 56$
$6:\ 67, 64, 65$
$7:\ 76$
$8:\ 84$

The PTDC:

$\overline{1} = \overrightarrow{12} = \overleftarrow{2}$
$\overline{2} = \overrightarrow{21, 13} = \overleftarrow{3}$
$\overline{3} = \overrightarrow{31, 14} = \overleftarrow{4}$
$\overline{4} = \overrightarrow{46, 65} = \overleftarrow{5}$
$\overline{5} = \overrightarrow{56} = \overleftarrow{6}$
$\overline{6} = \overrightarrow{67} = \overleftarrow{7}$
$\overline{7} = \overrightarrow{76, 64, 48} = \overleftarrow{8}$
$\overline{8} = \overrightarrow{84, 41} = \overleftarrow{1}$

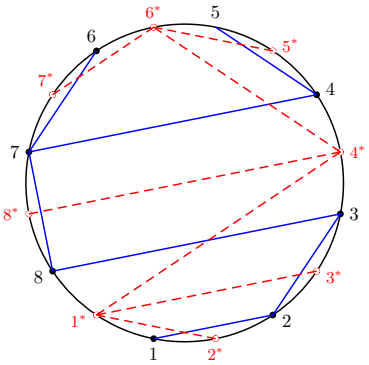

The LEO:

$1:\ 12$
$2:\ 21, 23$
$3:\ 32, 38$
$4:\ 47, 45$
$5:\ 54$
$6:\ 67$
$7:\ 76, 74, 78$
$8:\ 87, 83$

The PTDC:

$\overline{1} = \overrightarrow{12, 23, 38} = \overleftarrow{8}$
$\overline{2} = \overrightarrow{21} = \overleftarrow{1}$
$\overline{3} = \overrightarrow{32} = \overleftarrow{2}$
$\overline{4} = \overrightarrow{47, 78, 83} = \overleftarrow{3}$
$\overline{5} = \overrightarrow{54} = \overleftarrow{4}$
$\overline{6} = \overrightarrow{67, 74, 45} = \overleftarrow{5}$
$\overline{7} = \overrightarrow{76} = \overleftarrow{6}$
$\overline{8} = \overrightarrow{87} = \overleftarrow{7}$

FIGURE 11. Leos, PTDCs, and duality

lists coming from the PTDC of Γ^*, and vice versa. This can be seen in Fig. 11, the edges that constitute the trail starting at a given vertex are exactly the duals of the edges that are incident to that vertex.

Conversely, the peg can be recovered given the leo or the PTDC of the graph by gluing 2-cells to the graph in a procedure analogous to the way that one obtains a cellular embedding in a closed surface given a rotation scheme or a Cycle Double Cover. For example we can see in Fig. 11, that there is a half-disk attached to the tree along each trail of the PTDC. For details see [1, Section 4].

Pegs and their duality are closely related to factorizations of permutations into products of transpositions, indeed there is an obvious bijective correspondence[9] between factorizations of permutations of S_n into a product of m transpositions and edge-labeled graphs of size m with vertex set $[n]$, where as usual $n = m + 1$. Indeed such a factorization ρ can be viewed as a sequence of

[9] First observed by Dénes in [5].

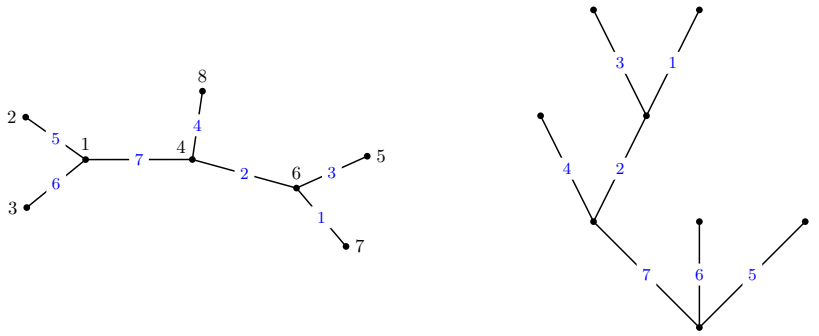

FIGURE 12. The e-v-tree (left) and the rooted e-tree (right) that corresponds to the factorization of our running example

m transpositions $\rho = (\tau_1, \ldots, \tau_m)$, and the corresponding graph has an edge labeled i connecting k and l if and only if $\tau_i = (k\,l)$. For example the e-v-tree that corresponds to the factorization $\rho = (6\,7), (4\,6), (5\,6), (4\,8), (1\,2), (1\,3), (1\,4)$ of the 8-cycle $(1\,2\,\ldots\,8)$ is shown in left side of Fig. 12. It is useful to consider factorizations up to conjugation (that is we consider factorizations (τ_i) and (τ_i^π) the same for any permutation π) and these correspond to e-graphs.

In fact, a factorization (or e-v-graph) determines a labeled peg, and an e-graph determines an unlabeled peg. Indeed the edge-labels induce a linear order of the edges which restricts to a linear order at the star of each vertex; equivalently the trajectories of the vertices determining a PTDC[10]. The mind-body duality then can be transferred to factorizations to define ρ^* and $\rho^{\bar{*}}$, and we have the following explicit formulas:[11]

$$\rho^* = \tau_1, {}^{\tau_1}\tau_2, \ldots, {}^{\tau_1 \cdots \tau_{m-1}}\tau_m \tag{2.3}$$

$$\rho^{\bar{*}} = \tau_1^{\tau_2 \tau_3 \cdots \tau_m}, \tau_2^{\tau_3 \cdots \tau_m}, \ldots, \tau_{m-1}^{\tau_m}, \tau_m. \tag{2.4}$$

For the factorization of our example, we have $\rho^* = (6\,7), (4\,7), (4\,5), (7\,8), (1\,2), (2\,3), (3\,8)$ and $\rho^{\bar{*}} = (7\,8), (5\,8), (5\,6), (1\,8), (2\,3), (3\,4), (1\,4)$, and we emphasize that these are factorizations of the inverse cycle $(8\,7\,\ldots\,1)$.

These formulas are best understood via the *Hurwitz action* of the braid group on factorizations. Recall that B_m, the braid group with m strands, is the group generated by $m-1$ generators $\sigma_1, \ldots, \sigma_{m-1}$ subject to the relations $\sigma_i \sigma_{i+1} \sigma_i = \sigma_{i+1} \sigma_i \sigma_{i+1}$, for $i = 1, \ldots, m-2$ and $\sigma_i \sigma_j = \sigma_j \sigma_i$ if $|i-j| \geq 2$. One of the basic incarnations of B_m is as a group of automorphisms of F_m the free group with m generators: if $x_1, \ldots, x_m$ are the generators of F_m then the action of the generator σ_i is given by $\sigma_i\, x_j = x_j$ for $j \neq i, i+1$, while $\sigma_i\, x_i = {}^{x_i}x_{i+1}$ and $\sigma_i\, x_{i+1} = x_i$. It follows that B_m acts on the right on the set of

[10] Alternatively we can obtain the peg as the total space of a branched covering of the disk, see [1, Section 4.4].

[11] Recall that we use left and right exponential notation for conjugation. Since transpositions are involutions the distinction is mute in the current context; however, it is useful in more general contexts.

homomorphisms $\mathrm{F}_m \to G$, for any group G and in particular for G a symmetric group. A factorization ρ is a sequence of elements in a symmetric group, and therefore can be construed as a representation of F_m to that group. So we have a right action of B_m on the set of all factorizations in any symmetric group, this action is called the *Hurwitz action*. If $\rho = \tau_1, \ldots, \tau_m$ is a factorization, then for the ith generator of B_m we have that $\rho\sigma_i = \tau'_1, \ldots, \tau'_m$, where $\tau'_i = {}^{\tau_i}\tau_{i+1}$, $\tau'_{i+1} = \tau_i$, and $\tau'_j = \tau_j$ for $j \neq i, i+1$.

The braid $\Delta_m = \sigma_1 \ldots \sigma_m \sigma_1 \ldots \sigma_{m-1} \ldots \sigma_1 \sigma_2 \sigma_1 \in \mathrm{B}_m$ is called the *Garside element* of B_m and it plays an important role in the theory of Braid Groups, for example it is a square root of the generator of the center of B_m. Its importance for the present work is that formulas (2.3) and (2.4) can be written as

$$\rho^* = (\rho\Delta_m)^{\mathsf{T}} \tag{2.5}$$

$$\rho^{\bar{*}} = \left(\rho\Delta_m^{-1}\right)^{\mathsf{T}}, \tag{2.6}$$

where for a factorization ρ, ρ^{T} stands for the factorization read backwards: if $\rho = (\tau_1, \ldots, \tau_m)$ then $\rho^{\mathsf{T}} = (\tau_m, \ldots, \tau_1)$.

Using the bijection between factorizations in S_n and e-graphs on $[n]$ we can transfer this to a B_m-action on the set of e-labeled graphs on $[n]$ with m edges. It is easily seen that if Γ is an e-v-graph then $\Gamma\sigma_i$ is obtained from Γ by interchanging the labels of the ith and $(i+1)$st edge and then "sliding" the $(i+1)$st edge along the ith, while $\Gamma\sigma_i^{-1}$ is obtained by interchanging the ith and $(i+1)$st labels and then sliding the ith edge along the $(i+1)$st. We interpret a slide of an edge along a non-adjacent edge to have no effect. This action on e-v-labeled graphs, which we also call the *Hurwitz action*, is shown in Fig. 13, where only the edges labeled i and $i+1$ are shown since the other edges are not affected.

Notice that this action descends at the level of e-labeled graphs (just forget the v-labels in Fig. 13). We will still call it the Hurwitz action since no confusion is likely to arise, and we use formulas (2.5) and (2.6) to define mind-body duality for labeled graphs.

For a fixed n-cycle ζ (say $\zeta = (1\,2\,\ldots\,n)$) denote by $\mathcal{F}_m$ the set of minimal transitive factorizations of ζ, or equivalently the set of e-v-trees with monodromy ζ, and by $\mathcal{E}_m$ the set of e-trees of size m. There is a commutative diagram of projections:

$$\begin{array}{ccc} \mathcal{F}_m & \xrightarrow{\;p\;} & \mathcal{N}_m \\ \downarrow & & \downarrow \\ \mathcal{E}_m & \xrightarrow{\;\bar{p}\;} & \widetilde{\mathcal{N}}_m \end{array} \tag{2.7}$$

where the vertical arrows are given by forgetting the v-labels and the horizontal by forgetting the e-labels and remembering only the leos they induce.

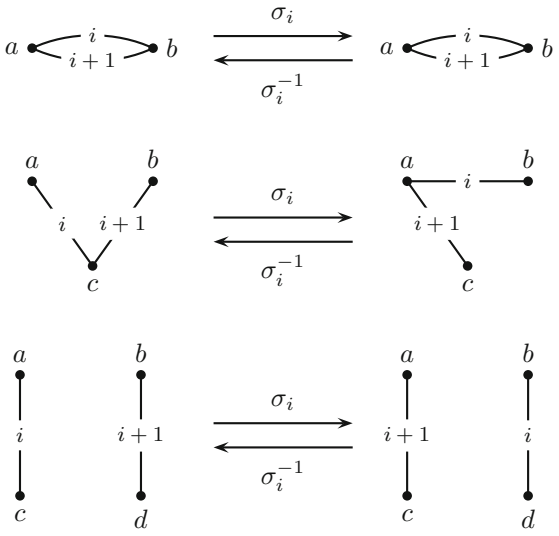

FIGURE 13. The Hurwitz action on e-v-graphs

The following theorem was proven in [19] and [9] independently. See the remarks about the proof of Proposition 2.24, for a proof using the theory of pegs.

Theorem 2.17. *Two factorizations belong to the same fiber of p if and only if they differ by a sequence of interchanges of consecutive commuting factors. In particular, the set of minimal transitive factorizations of an n-cycle, up to commutation of adjacent factors, is in bijection with $\mathcal{N}_m$, and is, therefore, counted by the $(p = 3)$ Fuss–Catalan numbers ν_m (see Eq. (1.2)).*

A single such interchange of, say, the ith and $(i + 1)$st factor, can be effected by the action of a braid generator σ_i, and since $\Delta_m \sigma_i = \sigma_{m-i} \Delta_m$ it follows that the action of Δ_m on $\mathcal{F}_m$ (respectively, $\mathcal{E}_m$) descends to a map $\kappa\colon \mathcal{N}_m \to \mathcal{N}_m$, (respectively $\tilde{\kappa}\colon \widetilde{\mathcal{N}}_m \to \widetilde{\mathcal{N}}_m$), and this map is the "dual" for nc-trees defined in [15]. It was proved in [1] that Δ_m^2, the central element of B_m, acts on an e-v-graph Γ by relabeling its vertices according to its monodromy $\mu(\Gamma)$, and trivially on an e-graph. Since the monodromy of an e-v-tree is a cycle we have that κ^2 is a rotation by $2\pi/n$ radians,[12] while $\tilde{\kappa}^2 = \mathrm{id}$. We will call $\kappa(t)$ the *complement* of t. The mind-body dualities $*, \bar{*}$ descend to maps $\mathcal{N}_m \to \mathcal{N}_m^{\mathsf{T}}$ and as a consequence of Eq. (2.5) we have that $\kappa(t) = (t^*)^{\mathsf{T}}$ and $\kappa^{-1}(t) = (t^{\bar{*}})^{\mathsf{T}}$.

We want to define (involutory) dualities

$$*, \bar{*}\colon \mathcal{N}_m \to \mathcal{N}_m$$

[12] What we called c in Remark 2.16.

that lift the mind-body duality for unlabeled trees, and as indicated in Section 5.2 of [1] this can be done by projecting the (pullback) of mind-body duality for rooted e-trees rather than for factorizations. We explain that next.

For any n-cycle $\zeta \in \mathrm{S}_n$ there is a bijection[13]

$$f_\zeta \colon \mathcal{F}^\zeta \to \mathcal{E}_m^*$$

from minimal factorizations of ζ to *rooted* e-trees with m edges. For a factorization ρ, $f_\zeta(\rho)$ is the rooted e-tree obtained from the corresponding e-v-tree by declaring the vertex labeled 1 to be the root and forgetting the vertex labels. Conversely given a rooted e-tree t its monodromy is a full cycle in $\mathcal{S}_V$ and once we label the root of t by 1 there is a unique way to label the rest of the vertices so that $\mu(t)$ becomes ζ. For example the rooted e-tree that corresponds to our example factorization of $(1\,2\,\ldots\,8)$ is shown in the right side of Fig. 12.

We can extend the braid action to rooted e-graphs by just letting the root stay the same, and so we can define mind-body dualities $*, \bar{*} \colon \mathcal{E}_m^* \to \mathcal{E}_m^*$, by Eqs. (2.5) and (2.6). It can be easily checked that the following diagram commutes:

$$\begin{array}{ccc} \mathcal{F}^\zeta & \xrightarrow{f_\zeta} & \mathcal{E}_m^* \\ {\scriptstyle *,\,\bar{*}}\downarrow & & \downarrow{\scriptstyle \bar{*},\,*} \\ \mathcal{F}^{\zeta^{-1}} & \xleftarrow{f_{\zeta^{-1}}^{-1}} & \mathcal{E}_m^* \end{array} \tag{2.8}$$

Using f_ζ^{-1} instead of $f_{\zeta^{-1}}^{-1}$ in the bottom row of this commutative diagram we obtain involutory dualities $\mathcal{F}^\zeta \to \mathcal{F}^\zeta$, and we can then project those to $\mathcal{N}_m$ to get involutory dualities that lift the duality of unlabeled nc-trees.

Definition 2.18. The *nc-dualities* $*, \bar{*} \colon \mathcal{N}_m \to \mathcal{N}_m$ are defined via the following commutative diagram:

$$\begin{array}{ccc} \mathcal{E}_m^* & \longrightarrow & \mathcal{N}_m \\ {\scriptstyle *,\,\bar{*}}\downarrow & & \downarrow{\scriptstyle \bar{*},\,*} \\ \mathcal{E}_m^* & \longrightarrow & \mathcal{N}_m \end{array} \tag{2.9}$$

where the horizontal arrows are $p \circ f_\zeta^{-1}$. From now on, unless explicitly mentioned, the term *duality*, in the context of nc-trees, will refer to these involutory dualities.

It is easy to see that $t^* = \overline{\kappa(t)}$, i.e. the nc-tree obtained by reflecting $\kappa(t)$ across the diameter that passes through the vertex labeled 1. For example the

[13] Essentially due to Moszowski [20].

nc-dual of the nc-tree on the left side of Fig. 2 is shown in the right side of Fig. 3. Since κ has order $2n$ we have:

Proposition 2.19. *Let $r, s, \kappa\colon \mathcal{N}_m \to \mathcal{N}_m$ stand for nc-duality, reflection across the diameter that passes through 1, and the complement, respectively. Then*

$$r = s \circ \kappa$$

and therefore the group generated by the involutions r, s is isomorphic to D_{2n} the dihedral group with $4n$ elements.

It turns out that $\mathcal{N}$ is a free $*$-magma, generated by the nc-tree λ consisting of a single vertex labeled 1 and no edges. This will be exposed in Sect. 2.7 after we have introduced in Sect. 2.6 the set $\mathcal{P}$ of *flagged Perfectly Chain Decomposed Ditrees*.

We end this subsection by introducing a bijection analogous to f_ζ between labeled nc-trees and a class of ordered trees in the next section, and explaining the connection of κ with the Kreweras complement in Sect. 2.5.2.

2.5.1. The Set of Bipartisan Trees. Recall that an *ordered tree* is a rooted tree where the children of every vertex have been given a linear order.

Definition 2.20. Let v be a non-root vertex in a rooted tree. The *trunk* of v is the last edge e_v in the unique path from the root to v.

A *bipartisan tree* is an ordered tree, where the children of every vertex are partitioned into two classes, the *left children* and the *right children*, in such a way that every left child is less than every right child.

The set of bipartisan trees with m edges is denoted by $\mathcal{BO}_m$.

Proposition 2.21. *There is a bijection $f\colon \mathcal{N}_m \to \mathcal{BO}_m$.*

Proof. Projecting Moszkowski's f_ζ gives a bijection from the set $\mathcal{N}_m$ to the set of rooted trees with leos. Now given a rooted tree with a leo, for a vertex v with trunk e_v let $l_1 < \cdots < l_k < e_v < r_1 < \cdots < r_s$ be the edges incident to v ordered according to the leo at v. Call $l_1, \ldots, l_k$ the left children and $r_1, \ldots, r_s$ the right children and put them in the order $r_1, \ldots, r_s, l_1, \ldots, l_k$ to obtain a bipartisan tree $f(t)$.

Conversely, given a bipartisan tree t we obtain the leo of a non-root vertex by listing first the trunks of the left children according to the order of the ordered tree, followed by the trunk of v, and finally listing the trunks of the right children again in the order given by the ordered tree. The edges incident to the root are ordered according to the order of their endpoints. □

See Fig. 14 as an example where the bipartisan tree corresponding to the nc-tree of Fig. 1 is shown, and the leo structure at every vertex is indicated by oriented arcs around that vertex.

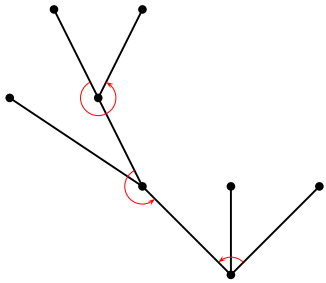

FIGURE 14. The bipartisan tree representing the nc-tree of Fig. 1

2.5.2. The Kreweras Complement on the Lattice of Non-crossing Partitions. The lattice of non-crossing partitions is well studied and we refer the reader to [2] for the basic definitions and the extensive bibliography. In this subsection we show that the map $\kappa\colon \mathcal{N}_m \to \mathcal{N}_m$ induced by the action of the Garside element on the set of rooted e-trees, has an interpretation in terms of the Kreweras complement on the lattice $\mathcal{NC}_n$ of non-crossing partitions of a set of n elements, where as usual $n = m + 1$.

Let $\mathcal{G} = \mathrm{Cay}(\mathrm{S}_n, T)$ be the Cayley graph of the symmetric group with respect to the generating set T of all transpositions. Define $\pi_1 \leq \pi_2$ if there is a geodesic path (with respect to the word length metric) in $\mathcal{G}$ from the identity to π_2 that passes through π_1. This gives a partial order in S_n called the *absolute order*. The lattice of non-crossing partitions $\mathcal{NC}_n$ is (isomorphic to) the interval $[\mathrm{id}, \zeta] \subset \mathrm{S}_n$ in the absolute order. This is a complemented lattice and one of its complements, the so called Kreweras complement, is given by the formula[14]

$$K(\pi) = \zeta\pi^{-1}.$$

There is a bijection between $\mathcal{C}$, the set of maximal chains in $\mathcal{NC}_n$ and $\mathcal{F}_m$ the set of minimal transitive factorizations of ζ. Indeed they both determine a geodesic path (i.e. a path of minimal distance) in $\mathcal{G}$ from id to ζ, and the labels of the vertices of that path give a maximal chain $c = (\mathrm{id} = \pi_0 < \pi_1 < \ldots < \pi_m = \zeta)$, while the labels of the edges give a factorization $\rho = \tau_1, \ldots, \tau_m$. More precisely, we have two inverse bijections:

$$\partial\colon \mathcal{C} \to \mathcal{F}_m, \quad c \mapsto \pi_0^{-1}\pi_1, \pi_1^{-1}\pi_2, \ldots, \pi_{m-1}^{-1}\pi_m$$

$$\int\colon \mathcal{F}_m \to \mathcal{C}, \quad \rho \mapsto \mathrm{id}, \tau_1, \tau_1\tau_2, \ldots, \tau_1\tau_2\ldots\tau_m.$$

Since K is an anti-isomorphism of $\mathcal{NC}_n$ it maps maximal increasing chains to maximal decreasing chains and we can define a map

$$\kappa\colon \mathcal{C} \to \mathcal{C}, \quad \kappa(c) = K(\pi_m), K(\pi_{m-1}), \ldots, K(\pi_1), K(\pi_0).$$

[14] This is different than the formula in [2]. The inconsistency is due to different conventions on how to multiply transpositions and how exactly the braid group acts. With our conventions Armstrong's formula would give K^{-1} that corresponds to the action of Δ_m^{-1}. Of course, K^{-1} is also a complement in the lattice.

It turns out that the action of the Garside element Δ_m is given by κ interpreted as a map between factorizations.

Proposition 2.22. *For a factorization ρ we have*

$$\rho\Delta = \partial\kappa\left(\int \rho\right).$$

Proof. If $\int \rho = \pi_0, \pi_1, \ldots, \pi_m$, then (see Eq. (2.5)) we have that

$$\rho\Delta = {}^{\pi_{m-1}}\tau_m, {}^{\pi_{m-2}}\tau_{m-1}, \ldots, {}^{\pi_1}\tau_2, {}^{\pi_o}\tau_1$$

and so since $\pi_j = \pi_{j-1}\tau_j$ for $j = 1, \ldots, m$ we see that

$$\int \rho\Delta = \mathrm{id}, {}^{\pi_{m-1}}\tau_m, {}^{\pi_{m-2}}(\tau_{m-1}\tau_m), \ldots, {}^{\pi_1}(\tau_2 \ldots \tau_m), {}^{\pi_0}(\tau_1 \ldots \tau_m) = \pi_m.$$

Now since $\zeta = \pi_m = \tau_1 \ldots \tau_m$ we have that

$$K(\pi_j) = \tau_1 \ldots \tau_m \tau_j \ldots \tau_1 = {}^{\pi_j}(\tau_{j+1} \ldots \tau_m).$$

Thus

$$\int \rho\Delta = \kappa\left(\int \rho\right)$$

as we needed. □

2.6. Perfectly Chain Decomposed Ditrees

The *medial digraph* of a peg Γ is the analogue of medial graphs in the theory of cellularly embedded graphs. Essentially the medial digraph of Γ is the digraph $\mathcal{M}(\Gamma)$ obtained by putting together the Hasse diagrams of all the local edge orderings: its vertices are the edges of Γ and there is an edge from e_1 to e_2 if and only if $e_1 \leq e_2$ in the leo of a vertex of Γ. Each edge of Γ is incident to two vertices and is preceded (or followed) by at most one edge at the leo of each of those vertices. It follows that the in and out degrees at every vertex of the medial digraph are at most 2. Conversely, every digraph that satisfies these degree restrictions is the medial digraph of a peg, see Item 2 in Proposition 2.24. For example in the top of Fig. 15 we see the medial digraphs of the pair of dual pegs of Fig. 11. Notice that the two medial digraphs are isomorphic and this is true in general: the map $e \mapsto e^*$ defines an isomorphism between the medial digraphs of dual pegs. The local linear order at the star of each vertex gives a chain in the medial digraph, and in Fig. 15 the chains that come from different vertices are indicated by different colors. We remark that the peg can be reconstructed from its medial digraph once this decomposition into chains is known. This observation is important for what follows so we develop it in some detail.

Definition 2.23. A *medial digraph* is a digraph with the in and out degrees of all vertices at most two. A *Perfect Chain Decomposition* (*PCD* for short) of a medial digraph is a decomposition $\mathcal{C}$ of its edges into chains with the property that every vertex belongs to exactly two chains. We emphasize that chains of

length zero consisting of a single vertex are allowed[15]. For a chain $c \in \mathcal{C}$ we use the notation $\alpha(c)$ (resp. $\omega(c)$) to stand for the first (resp. last) vertex of c.

A vertex of a medial digraph is called *internal* if both its in and out degree are at least 1. Notice that constructing a PCD on a medial digraph d involves a binary choice at every internal vertex, namely which incoming edge to connect to which outgoing edge. The *dual* $\mathcal{C}^*$ of a PCD $\mathcal{C}$ is the PCD obtained from $\mathcal{C}$ when the opposite choice of such connections is made at every internal vertex.

The following summarizes the main results for PCDs on medial digraphs from [1]:

Proposition 2.24. *We have:*

1. *The Euler characteristic of* $\mathcal{M}(\Gamma)$ *equals the Euler characteristic of* Γ. *In particular for a non-crossing tree* t *we have that the underlying graph of* $\mathcal{M}(t)$ *is a tree.*
2. *The leo of a peg* Γ *induces a PCD on its medial digraph* $\mathcal{M}(\Gamma)$, *and the peg can be reconstructed from that PCD.*
3. *Mind-body dual pegs have isomorphic medial digraphs and they induce dual PCDs.*
4. *A peg* Γ *comes from a factorization if and only if its medial digraph is a dag.*[16] *In particular, by Item 1, any leo on a tree comes from a factorization.*

Remarks on the proof. For detailed proofs consult [1]. Regarding Item 2, the peg that corresponds to a PCD $\mathcal{C}$ on a medial digraph d has a vertex v_c for any chain $c \in \mathcal{C}$ and each vertex w of d gives an edge e_w connecting v_{c_1} and v_{c_2} where c_1 and c_2 are the two chains that w belongs to. Clearly an edge e_w belongs to the star of a vertex v_c if and only if w is contained in c, and so the order of the vertices of c gives a linear order at the star of each vertex endowing the resulting graph with a leo.

In the bottom half of Fig. 15 we see the PCDs on the medial ditrees[17] of the pair of mind-body dual nc-trees of Fig. 11. When drawing medial ditrees we omit arrows and use the convention that all edges are directed upwards, and we follow the same convention when we draw the chains of a PCD.

Regarding Item 4, notice that the edges of a peg that comes from a factorization are totally ordered by their labels, and that order gives a *topological sort* in its medial digraph[18]. Actually the set of all possible factorizations (up to conjugation) that give that peg is in bijection with the set of topological sorts of its medial digraph. We remark that it is relatively easy to prove (see for example [28]) that any two topological sorts of a dag differ by a sequence of adjacent transpositions, and this can be used to prove Theorem 2.17. □

[15] Actually when Γ is a tree they are required!

[16] Directed Acyclic Graph. This observation is essentially due to [8]. The definition of medial digraphs was inspired in part from that paper.

[17] Recall that a ditree is a digraph whose underlying graph is a tree.

[18] That is a *linear extension* of the poset whose Hasse diagram is the dag.

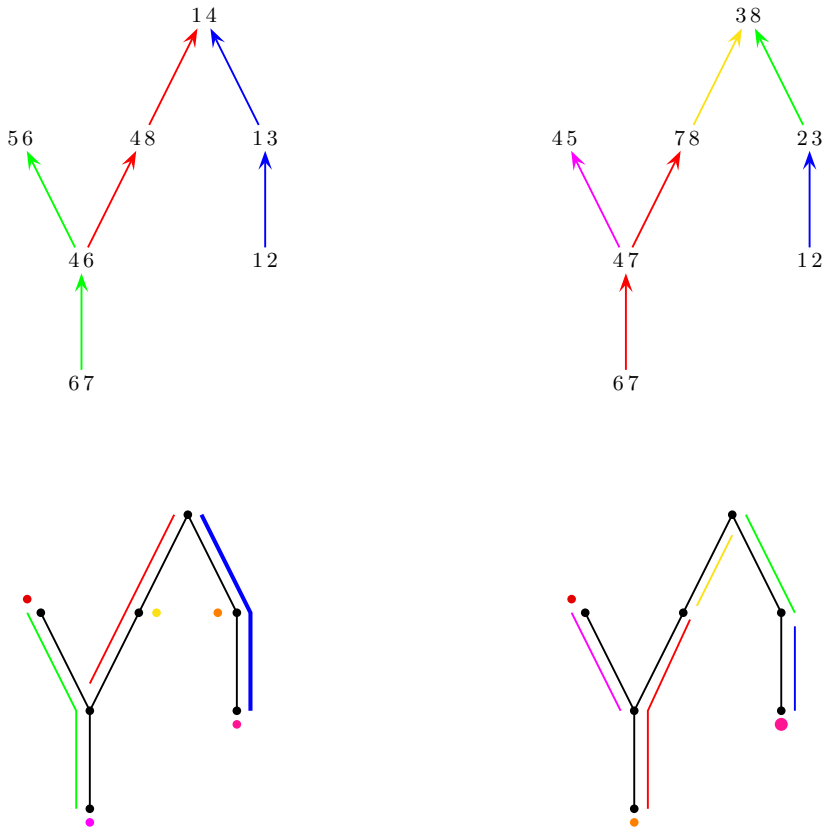

FIGURE 15. The PCDDs of the non-crossing trees of Fig. 11

By Proposition 2.24 we can encode unlabeled nc-trees and their duality with medial ditrees endowed with a PCD. This encoding can be extended to labeled nc-trees by encoding one additional piece of information: which chain of the PCD corresponds to the vertex labeled 1.

Definition 2.25. A *Perfectly Chain Decomposed Ditree* (*PCDD* for short) is a medial ditree endowed with a PCD and a *Flagged Perfectly Chain Decomposed Ditree* is a PCDD endowed with a distinguished chain called its *flag*.

We will use the same symbol (typically d) to denote the PCDD and its underlying medial ditree, and in that case the flag will be denoted by $f(d)$. For a chain $c \in \mathcal{C}$ we use the notation $\alpha(c)$ (resp. $\omega(c)$) to stand for the first (resp. last) vertex of c, and for a flagged PCDD d we use the notation $\alpha(d)$ and $\omega(d)$ to stand for $\alpha\left(f(d)\right)$ and $\omega\left(f(d)\right)$ respectively.

The set of flagged PCDDs with m vertices will be denoted by $\mathcal{P}_m$ and the set of (unflagged) PCDDs with m vertices by $\widetilde{\mathcal{P}}_m$ and we let $\mathcal{P} = \bigcup_{m\geq 0} \mathcal{P}_m$, and $\widetilde{\mathcal{P}} = \bigcup_{m\geq 0} \widetilde{\mathcal{P}}_m$.

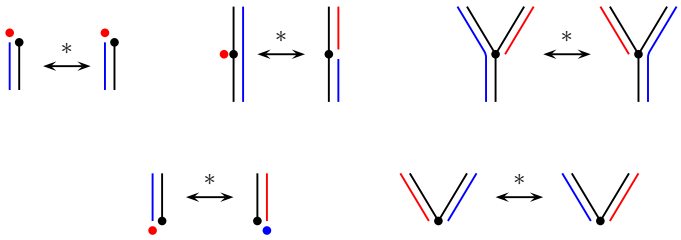

FIGURE 16. The flag of the dual of a flagged PCD

The *reverse* $\bar{d}$ of a PCDD d is the PCDD whose underlying ditree is the reverse ditree, its chains are the reverses of the chains of d, and its flag is the reverse of the flag of d.

For a flagged PCDD d, d^* is also flagged and its flag f^* is defined as follows: $\alpha(f^*) = \alpha(f)$ and if f is the only chain that starts at $\alpha(f)$ then f^* is the only chain of d^* that starts at $\alpha(f)$, otherwise the first edge of f^* is the outgoing edge incident at $\alpha(f)$ that does not belong to f, if no such edge exist then f^* is a trivial chain. All possible local configurations are shown in Fig. 16, the flags of the relevant PCDs are shown in red.

We extend the definition of PCDD to include the following two degenerate[19] cases that correspond to the nc-trees with 0 and 1 edges:

- The *empty PCDD* λ is the triple $(\emptyset, \{\emptyset\}, \emptyset)$ consisting of the empty ditree, the perfect chain decomposition consisting of the empty chain, and the empty chain as flag. The functions α and ω are not defined for the empty flag, and therefore not for λ either.
- The *point PCDD* $\mathfrak{p}$ is the triple $(p, \{p, p\}, p)$, consisting of a ditree with one vertex and no edges, a chain decomposition consisting of two identical trivial chains, and the unique chain as a flag.

We summarize the above discussion in the following theorem, for more details see Section 5 of [1].

Theorem 2.26. *The function*

$$\mathcal{M}\colon \mathcal{N}_m \to \mathcal{P}_m$$

that assigns to an nc-tree t its medial ditree endowed with the PCD induced by the leo of t and having as flag the chain that corresponds to the leo of the vertex labeled 1 *is a duality-preserving bijection.*

We now exhibit $\mathcal{P}$ as a free $*$-magma. In what follows PCDD will always mean a *flagged PCDD*.

Definition 2.27. Let $d_{\mathrm{l}}, d_{\mathrm{m}}, d_{\mathrm{r}}$ be PCDDs. Their *fusion* is defined to be the PCDD $\Upsilon(d_{\mathrm{l}}, d_{\mathrm{m}}, d_{\mathrm{r}})$ where:

[19] The first one may even be called pointless.

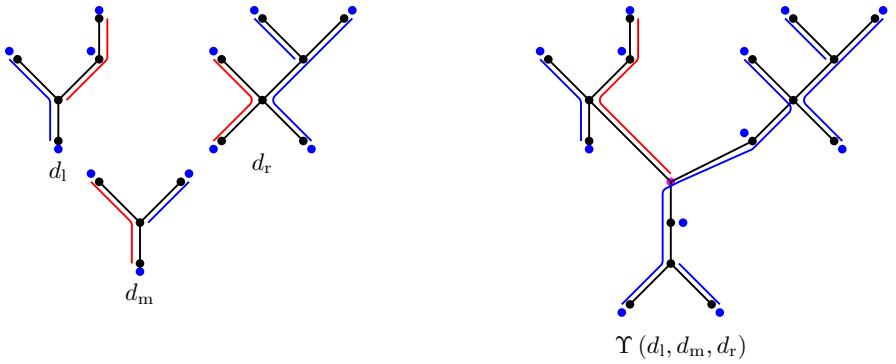

FIGURE 17. An example of the fusion of PCDDs

- The underlying ditree has as vertices the (disjoint) union of the vertices of $d_\mathrm{l}, d_\mathrm{m}, d_\mathrm{r}$, plus a new vertex v_0. The edges are the edges of $d_\mathrm{l}, \overline{d}_\mathrm{m}, d_\mathrm{r}$ plus, provided that the corresponding flags are not empty, edges connecting v_0 to $\alpha(d_\mathrm{l})$ and $\alpha(d_\mathrm{r})$ and an edge connecting $\omega(\bar{d}_\mathrm{m})$ to v_0.
- The chains are the non-flag chains of d_l, $\overline{d}_\mathrm{m}$ and d_r, and two additional chains: $f(\overline{d}_\mathrm{m}) \to v_0 \to f(d_\mathrm{r})$, and $v_0 \to f(d_\mathrm{l})$.
- The flag is $v_0 \to f\,(d_\mathrm{l})$.

Notice that with this definition $\Upsilon(\lambda, \lambda, \lambda) = \mathfrak{p}$. A less trivial example of the fusion of three PCDDS is shown in Fig. 17, the flag of each PCDD is indicated in red.

Theorem 2.28. *With the above definitions $\mathcal{P}$ is a free $*$-magma.*

Proof. Starting with a non-empty PCDD d and removing $\alpha(d)$ we obtain three PCDDs: d_l induced by those vertices of d that are above $\alpha(d)$ and were connected to $\alpha(d)$ by the first edge of f, d_m the inverse of the PCDD induced by the vertices of d that are below $\alpha(d)$, and d_r induced by the remaining vertices. Clearly $d = \Upsilon(d_\mathrm{l}, d_\mathrm{m}, d_\mathrm{r})$, and since d is finite it is clear that by recursively continuing this process we will eventually find an expression for d that consists of applications of Υ and λ, and that such an expression is unique. So $\mathcal{P}$ is a ternary magma freely generated by λ.

To follow the proof that Eq. (2.2) is satisfied the reader may want to consult Fig. 18, where the dual of $\Upsilon(d_\mathrm{l}, d_\mathrm{m}, d_\mathrm{r})$ of Fig. 17 is shown as the fusion of d_l^*, d_m^*, and d_r^*. We first note that the underlying ditrees of both sides of the equation are equal. We need to prove that at every vertex the same choice of connections is made, and this is clear for vertices different than v_0, $\alpha(d_\mathrm{l})$, $\alpha(\overline{d_\mathrm{m}})$, and $\alpha(d_\mathrm{r})$ since switching the connections can be done either before or after fusing the PCDDs. Switching the connections of $\Upsilon(d_\mathrm{l}, d_\mathrm{m}, d_\mathrm{r})$ at $\alpha(\overline{d_\mathrm{m}})$ means that we connect $f(\overline{d_\mathrm{m}}^*)$ to v_0 and by switching at v_0 the resulting chain continues by connecting v_0 to $f(d_\mathrm{l}^*)$. By definition the same choices of connections are made in the construction of $\Upsilon(d_\mathrm{r}^*, d_\mathrm{m}^*, d_\mathrm{l}^*)$. Similarly, one can easily see that the flags of the two sides also agree. □

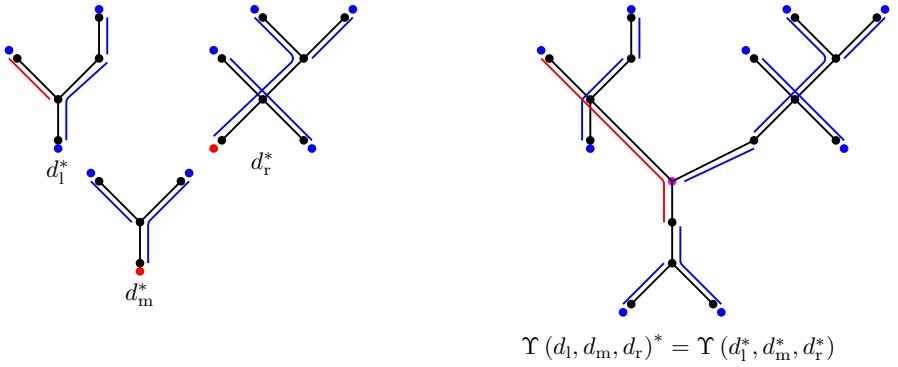

FIGURE 18. The dual of Fig. 17

2.7. $\mathcal{N}$ as a Free $*$-Magma

We use the bijection $\mathcal{M}$ of Theorem 2.26 to endow $\mathcal{N}$ with the structure of a free ternary magma generated by the nc-tree with one vertex λ, i.e. so that $\mathcal{M}$ is the structural bijection. Since $\mathcal{M}$ is duality-preserving this exhibits $\mathcal{N}$ endowed with nc-duality as a free $*$-magma.

Given an nc-tree t let $1\,k$ be the rightmost edge incident to 1. Removing that edge gives a forest of two nc-trees the one attached to k and the one attached to 1, t_{l} is the latter, t_{m} is the tree to the left of $(1, k)$ and t_{r} the one to the right, see Fig. 22.

Conversely given three nc-trees t_{l}, t_{m}, and t_{r} of orders n_1, n_2, and n_3 respectively, their fusion $\Upsilon\left(t_{\mathrm{l}}, t_{\mathrm{m}}, t_{\mathrm{r}}\right)$ is obtained by relabeling the vertex 1 of t_{r} as $n_3 + 1$, relabeling t_{m} by $i \mapsto i + n_3$, and finally t_{l} by $i \mapsto i + n_2 + n_3 - 1$ except that we keep the label of 1. Notice that the roots of t_{m} and t_{r} receive the same label $n_3 + 1$ so we identify them. Finally we add an edge connecting 1 and $n_3 + 1$.

As an example, the nc-trees that correspond to the PCDDs of the example in Fig. 17, and their fusion are shown in Fig. 19.

3. The Structural Bijections

In this section, we give combinatorial/topological interpretations of the structural bijections in Diagram (1.3).

3.1. The Structural Bijection $\psi\colon\ \mathcal{Q} \to \mathcal{T}$

A nice topological/combinatorial description of $\psi\colon\ \mathcal{Q}_m \to \mathcal{T}_m$ has been given in [16]. For a quadrangular dissection q, $\psi(q)$ is a sort of dual of q viewed as a graph embedded in the disk with all its vertices mapped on the boundary circle: the disk is divided into $n - 1$ quadrangular cells (the cells of the dissection q) and $2n$ bigons formed by the edges of the polygons and the arcs of the boundary circle. Let T be the 4-valent plane tree that has a vertex for each of these regions, and an edge between two vertices if the corresponding regions

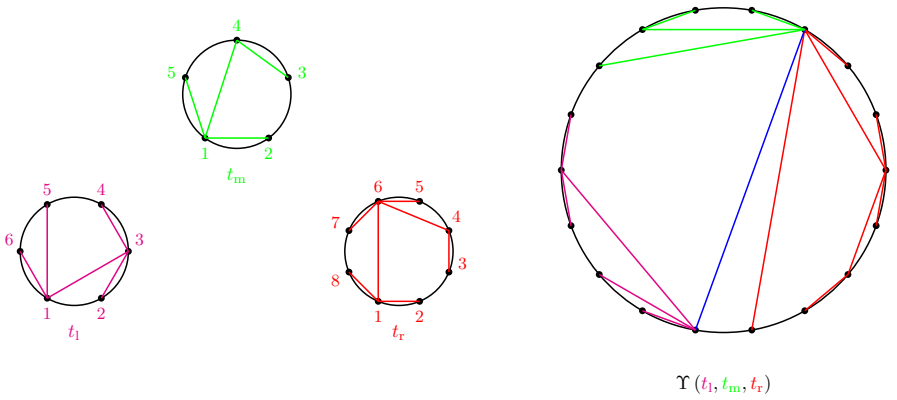

FIGURE 19. The nc-trees corresponding to the PCDDs of Fig. 17

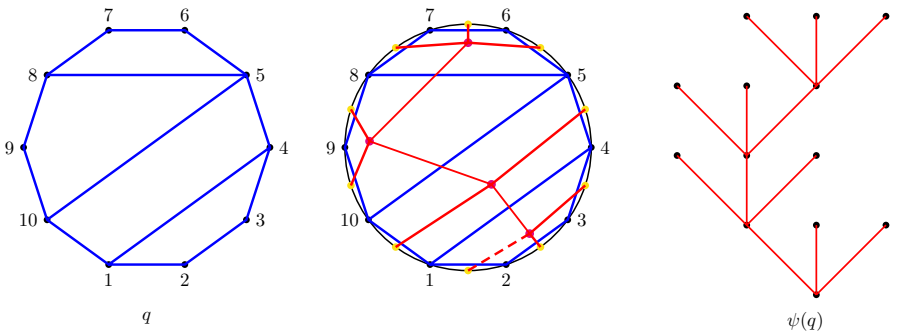

FIGURE 20. The construction of $\psi\colon\ \mathcal{Q}_m \to \mathcal{T}_m$

share an edge. See Fig. 20, where, in the middle, a vertex that corresponds to a cell is drawn in the interior of that cell, and a vertex that corresponds to a bigon is drawn in the boundary arc of that bigon. Clearly bigons give leaves of T and cells give internal vertices. The ternary tree $\psi(t)$ is obtained from T by removing the leaf that comes from the bigon that contains the root edge $1\,2$, declaring the vertex it was attached to the root of the remaining tree, and using the orientation of the disk to order the children of any internal vertex. See Fig. 20 for an example of this construction.

Clearly this process of obtaining $\psi(q)$ can be reversed: starting with a ternary tree t with m internal vertices construct an 4-valent plane tree T with $n := m+1$ vertices by attaching a new leaf labeled 1 2 below the root. Then list the leaves of T in the order induced by the counterclockwise orientation (starting at 1 2) and label them by the edges of the $2n$-gon in the order $1\,2, 2\,3, \ldots, 2n\ 1$, and label the corresponding pendant edges by the same label. Since t has $2n+1$ leaves and only $n-1$ internal vertices there is at least one internal vertex with all its children being leaves; if such a vertex has children labeled (from right to left) $i\ i+1, i+1\ i+2, i+2\, i+3$, label it $i\ i+1\ i+2\ i+3$

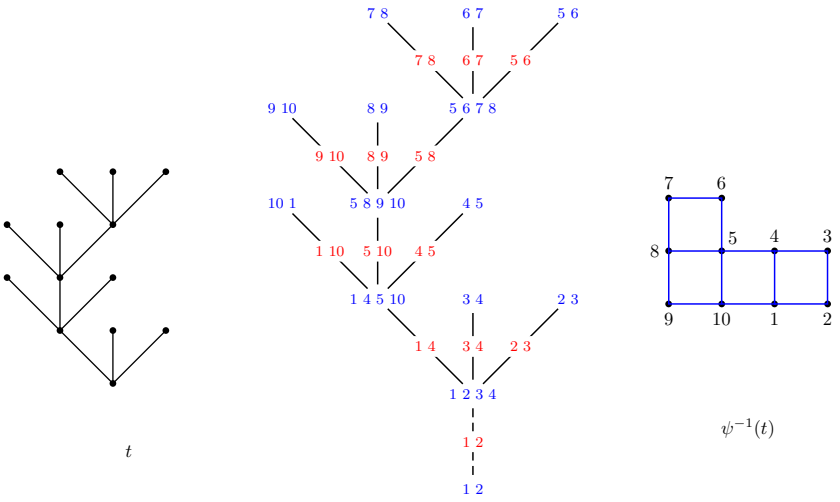

FIGURE 21. The construction of $\psi^{-1}\colon \mathcal{T}_m \to \mathcal{Q}_m$

and the the edge connecting it to its parent i $i+3$. Proceeding recursively we can label all internal vertices of T with the vertices of a quadrangular cell, and all non-pendant edges of T with a diagonal of the $2n$-gon. From this decorated tree we can reconstruct the n-cluster that corresponds to the polygonal dissection, for an example see Fig. 21, where we show $\psi^{-1}(t)$ for the ternary tree at the bottom right of Fig. 20.

Note that the above description of $\psi^{-1}(t)$ can be expressed in terms of the operation that t induces on ternary magmas described in Remark 2.10. Indeed, the label of an internal vertex of the intermediate tree T is obtained by applying the ternary operator $\mathrm{S}_n^3 \to \mathcal{S}_n\colon (a,b,c) \mapsto abc$ to its children viewed as transpositions. If we instead apply the ternary operator $\mathrm{S}_n^3 \to \mathcal{S}_n\colon (a,b,c) \mapsto c^{ba}$, and then push the label of every vertex to its trunk we obtain the labels of the edges.

3.2. The Structural Bijection $\sigma\colon \mathcal{N} \to \mathcal{T}$

The structural bijection $\sigma\colon \mathcal{N} \to \mathcal{T}$ is, modulo some choices, the bijection defined in Lemme 3.11 of [8]. Indeed the authors there define a bijection recursively by making an arbitrary choice of one of the six bijections $\mathcal{N}_2 \to \mathcal{T}_2$ and then for $t \in \mathcal{N}_m$ with $m > 2$ they recursively define the image of t to be $\Upsilon(t_{\mathrm{l}}, t_{\mathrm{m}}, t_{\mathrm{r}})$, where t_{l}, t_{m}, and t_{r} are defined, taking into account the difference in conventions, as in the second paragraph of Sect. 2.7, see Fig. 22. It follows that if we choose the structural bijection when $m = 2$ their bijection is exactly σ.

Since $\sigma = \psi \circ \phi^{-1}$ this work provides a combinatorial/topological interpretation of their bijection.

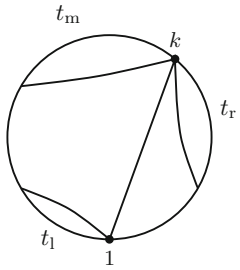

FIGURE 22. Expressing an nc-tree as $\Upsilon(t_{\mathrm{l}}, t_{\mathrm{m}}, t_{\mathrm{r}})$

3.3. The Structural Bijection $\phi\colon \mathcal{Q} \to \mathcal{N}$

Let q be a quadrangular dissection with m cells, then the polygon has $2n$ vertices where $n = m + 1$ and there are $m - 1$ diagonals. Since there are $2n$ vertices and $n-1$ cells, there is at least one cell with boundary containing three edges of the polygon. By inductively removing such extremal cells one can see that each dissecting diagonal connects two vertices of opposite parity, and so each cell has a diagonal that connects two odd vertices and a diagonal that connects two even vertices. The non-crossing tree $\phi(q)$ is the tree obtained by taking the "odd" diagonals of the cells, deleting the even vertices, and relabeling the odd vertices via $2i - 1 \mapsto i$. Since each edge of $\phi(q)$ is contained in a cell of the quadrangulation this is indeed an nc-tree.

To obtain $\phi^{-1}(t)$, for a non-crossing tree t, start by pegging t on the disk with vertices labeled $1, 3, \ldots, 2n - 1$, and construct $\kappa(t)$ with vertices labeled $2, 4, \ldots, 2n$. An edge e of t intersects only its dual edge e^* in $\kappa(t)$ and so we can construct a quadrangular cell by connecting their endpoints, if $e = i\,j$ with $i < j$ and $e^* = k\,l$ with $k < l$ we get the quadrangular cell $i\,k\,j\,l$ of $\phi^{-1}(t)$. See Fig. 23, for an example of this construction.

To see that the above construction does indeed give the structural bijection $\mathcal{Q} \to \mathcal{N}$, notice that this is obviously true for $m = 0, 1$ and, as shown in Fig. 22, the ternary operations agree.

It turns out that ϕ is not only duality-preserving but also equivariant with respect to the respective dihedral group actions (see Proposition 2.19 for the action of the dihedral group D_{2n} on $\mathcal{N}_m$).

Indeed, notice that the analogous construction using even diagonals will give $\kappa(\phi(q))$, thus showing that κ is the pushforward of rotation by π/n. Notice also that $r_{1\,2}$, the reflection across the perpendicular bisector of the root edge $1\,2$, interchanges "even" and "odd" diagonals, and maps the vertex labeled i to the vertex labeled $2n + 3 - i \pmod{2n}$, so that $2i - 1$ (the label of the ith vertex of t) is mapped to $2(n + 2 - 1)$ (the label of the i^*th label of t^*). Thus r is the pushforward of $r_{1\,2}$. So we have:

Theorem 3.1. *The bijection ϕ is D_{2n}-equivariant.*

3.3.1. Relation of ϕ to Schaeffer's Bijection. The bijection ϕ is closely related to a bijection between rooted quadrangulations of the plane with m faces

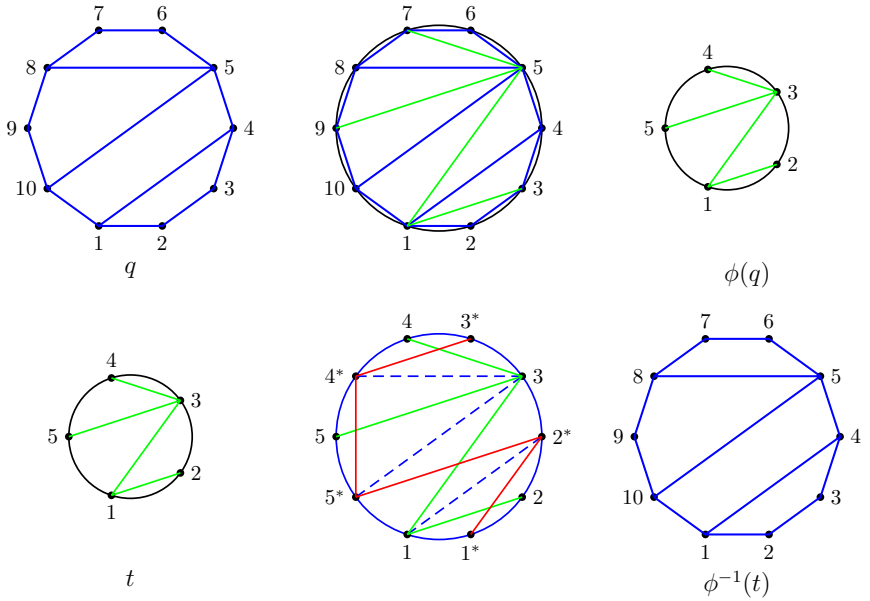

FIGURE 23. The construction of $\phi\colon\ \mathcal{Q}_m \to \mathcal{N}_m$ (top) and its inverse (bottom)

and well-labeled trees with m edges defined in [29] (see also [3]). A *rooted quadrangulation* is a map of the sphere Q where every face has degree 4, together with a distinguished *oriented* edge on the boundary of the unbounded face called the *root edge*. The starting vertex of the root edge of Q is called the *root*. A *well-labeled tree* is an ordered tree with its vertices labeled by positive integers in such a way that the labels of two adjacent vertices differ at most by one and the root is labeled 1.

The Schaeffer bijection S is defined as follows: let Q be a rooted quadrangulation. Start by labeling the vertices of Q with their distance from the root vertex v_0. Around every face of Q there is at least one pair of opposite vertices with the same label. Call a face *simple* if only one pair of opposite vertices has the same labels, and *confluent* otherwise. The image of Q is obtained by taking the diagonal connecting the two vertices with the maximum degree for confluent faces, while for a simple face f we select the edge incident to the vertex with maximal label that is leaving f on its left. The root of $S(Q)$ is the first edge incident to the endpoint of the root of Q, counterclockwise starting from the root of Q.

To express ϕ in terms of S we construct a rooted quadrangulation of the plane associated with a rooted quadrangular dissection q of a $2n$-gon by adding an extra vertex at a point in the exterior of the polygon and connecting it by an edge to all the even vertices. When we compute the distances from the new vertex, the even vertices are at distance 1 and the odd vertices at distance 2. So all the cells of q are confluent faces, and all the new faces simple. Therefore

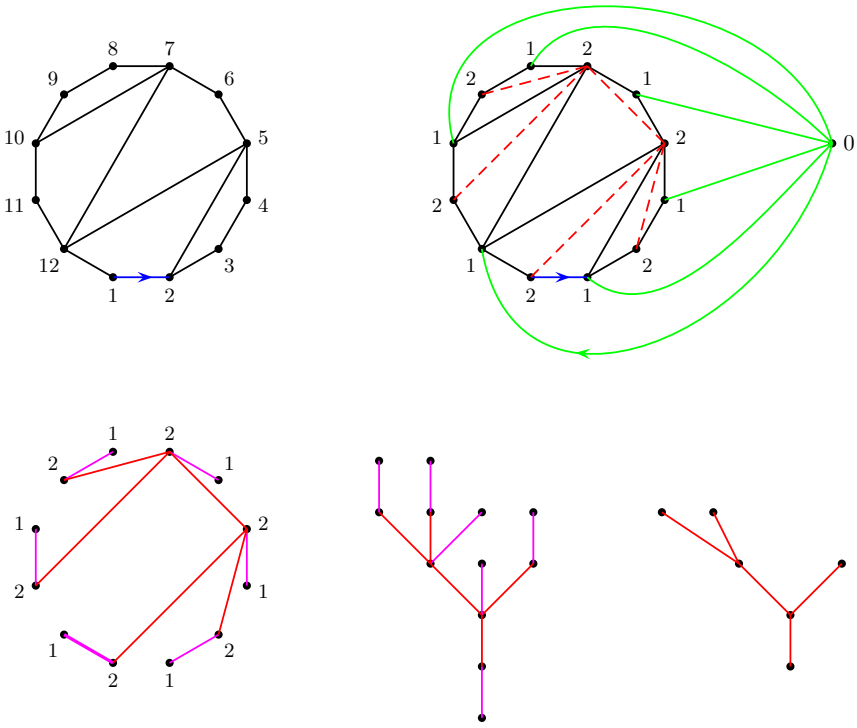

FIGURE 24. ϕ in terms of Schaeffer's bijection

each cell of q contributes its odd diagonal to the resulting wel-labeled tree, while each of the new faces contributes the leftmost of the sides of the polygon in its boundary. The result is a well-labeled tree where all internal vertices have label 2, all leaves have label 1 and each internal vertex is adjacent to exactly one leaf. Such trees are in bijection with bipartisan trees, just delete all leaves and use their position as a marker where the right children of every non-root internal vertex end, and where the left children begin. In Fig. 24 we carry out this construction for the quadrangular dissection of Fig. 9, the odd nc-tree is shown in red, and the contributions of the new faces in magenta. Clearly the nc-tree that corresponds to the bipartisan tree obtained this way is $\phi(q)$.

I would like to thank the anonymous referee of a previous version of this paper for bringing this connection to my attention and providing the construction from quadrangular dissections of a polygon to quadrangulations of the plane.

4. Enumerations

Next we take a closer look at the action of the dihedral group D_{2n} on $\mathcal{Q}_m$, where as usual $n = m + 1$. If κ stands for the rotation by $\frac{\pi}{n}$ radians, and r for

the reflection across the bisector of the root edge 1 2 then

$$\mathrm{D}_{2n} = \left\{\kappa^i r^j : i = 0, \ldots, 2n-1, \;\; j = 0, 1\right\}$$

and the elements with $j = 0$ and $i \neq 0$ are (counterclockwise) rotations, those with $j = 1$ are reflections, while, of course, $i = j = 0$ gives the identity. In particular $s = \kappa r$ is a reflection with axis that passes through the vertex labeled 1. Since $2n$ is even there are two conjugacy classes of reflections: those whose axis passes through two diametrically opposite vertices, and those whose axis passes through the midpoints of two diametrically opposite edges. The first class is represented by s and the second by r.

Notice that the subgroup $\langle \kappa^2, s \rangle$ is isomorphic to D_n, and the restriction of the D_{2n}-action on $\mathcal{Q}_m$ on that subgroup is carried by the structural bijection ϕ to the standard action of D_n on $\mathcal{N}_m$, where κ^2 is rotation by $\frac{2\pi}{n}$ radians and s is the reflection across the diameter that passes through 1, see Proposition 2.19 and Theorem 3.1.

The basic result of this section expresses the number of fixed points of elements of D_{2n} in terms of the number of self-dual elements of $\mathcal{A}$ of rank m (see Theorem 2.8), and thus, ultimately, in terms of Raney numbers.

Theorem 4.1. *Every reflection in* D_{2n} *fixes* s_m *elements of* $\mathcal{Q}_m$*. Rotation by* π *radians has* $(m+1)s_m$ *fixed points if* m *is even, and* $\frac{(m+1)s_m}{2}$ *if* m *is odd. When* $m \equiv 1 \pmod 4$*, rotations by* $\pm\frac{\pi}{2}$ *have* $\frac{m+1}{2} s_{\frac{m-1}{2}}$ *fixed points. No other rotation has fixed points.*

Proof. The basic observation is that the center of the polygon is fixed by all rotations and reflections, and for a quadrangular dissection q of a $2n$-gon fixed by an element of D_{2n} we have two cases: the center is in the interior of a cell or it is the midpoint of a dissecting diagonal (which then has to be a diameter of the circumscribed circle) of q, and that cell or dissecting diagonal then has to be invariant.

We first examine rotations. If the center is on a dissecting diameter, then since all dissecting diagonals connect vertices of opposite parity, this can happen if and only if m is even. This diameter has to be invariant under the rotation and it follows that the rotation is by π radians. Then q consists of two dissections (one a rotation by π of the other) of the $(n+1)$-gon, glued together along an edge. See Fig. 25 for an example of a rotation invariant dissection of an octadecagon: the diameter 1 10 is a dissecting diagonal, and q consists of a dissection of a decagon, glued along an edge to its rotation.

There are $n = m + 1$ diameters that could be dissecting diagonals, and there are $\nu_k = s_m$ dissections of the $(n+1)$-gon, where $m = 2k$. It follows that the central rotation by π has $(m+1)s_m$ fixed points, and no other rotation has fixed points.

If on the other hand the center belongs to an invariant cell, then the two diagonals of the cell are diameters and the rotation either fixes them or rotates one into the other. In the first case we have rotation by π and in the second by $\frac{\pi}{2}$. The number of cells that are to the south or east of the invariant cell equals the number of cells to the west or north, and thus there is an odd number of

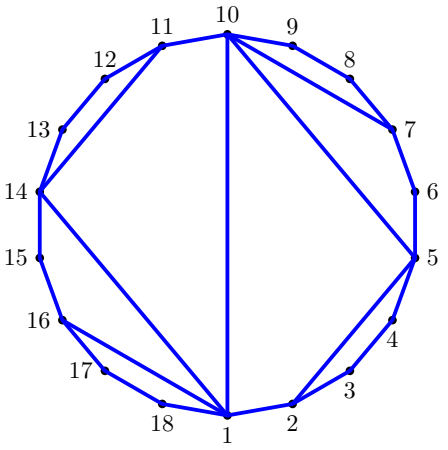

FIGURE 25. A rotation invariant quadrangular dissection of the octadecagon

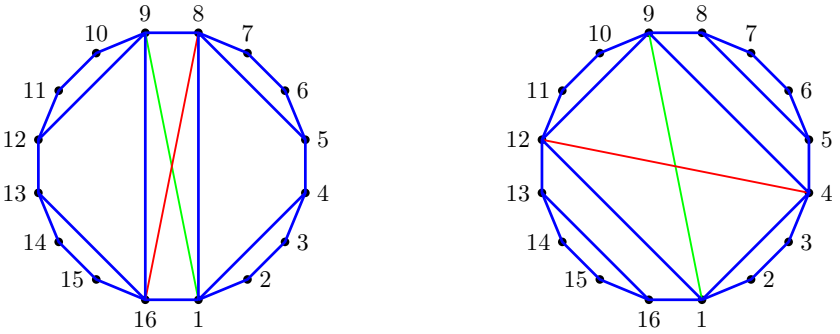

FIGURE 26. Quadrangular dissections of the hexadecagon invariant under rotation

total cells. It follows that this case occurs only when m is odd. For a dissection invariant under rotation by π radians one can see that it consists of a pair of smaller dissections (not necessarily both non-empty), one to the south which rotates to the one in the north, and one to the east that rotates to the one on the west. See Fig. 26 for two examples in the case $m = 7$.

It follows that for a given invariant cell, there are as many invariant dissections as pairs of dissections with total number of cells equal to $\frac{m-1}{2}$, which is counted by s_m. Now an invariant cell is determined by a pair of invariant diagonals (the two dual edges of the pair of dual non-crossing trees) and there are $\frac{m+1}{2}$ such pairs of dual edges.

Thus rotation by π has $\frac{(m+1)s_m}{2}$ fixed points.

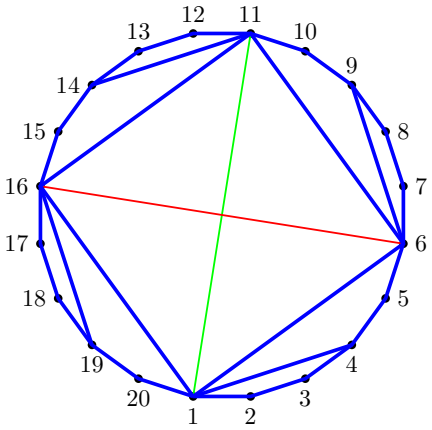

FIGURE 27. A quadrangular dissection of the icosagon invariant under rotation by $\frac{\pi}{2}$ radians

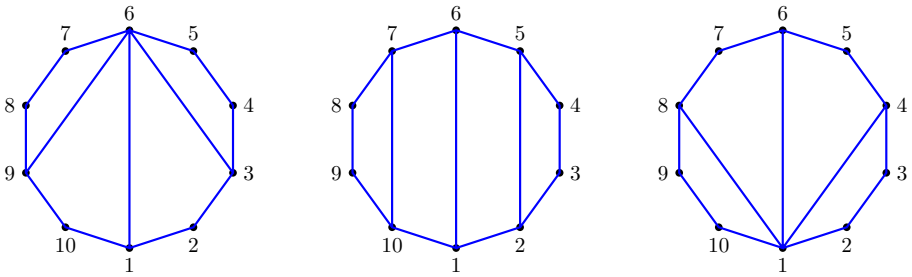

FIGURE 28. The three dissections of the decagon invariant under under reflection across 1 6

Notice that if $m = 2k-1$ with k odd, those pairs that consist of two equal dissections, are also invariant under rotation by $\pm\frac{\pi}{2}$, see for example Fig. 27 for a dissection of a dodecagon invariant under rotation by $\frac{\pi}{2}$.

The analysis for dissections invariant under a reflection is analogous. There are two conjugacy classes of reflections in D_{2n}: those whose axis passes through two diametrically opposite vertices, and those whose axis passes through the midpoints of two diametrically opposite edges. The second conjugacy class is represented by r and has been dealt with in Theorem 2.8.

For a reflection whose axis passes through two diametrically opposite vertices, we observe that if m is even, there can be no invariant cell (because there is an even number of them) and so the axis of reflection is a dissecting diagonal. The whole dissection then consists of a dissection of an $(m+2)$-gon glued to its reflection along an edge. So there are $\nu_{\frac{m}{2}} = s_m$ invariant dissections, for each of the $m+1$ diameters. For example, Fig. 28 displays the three dissections of a decagon that are invariant under reflection across the axis 1 6.

If m is odd, because we have an odd number of cells, the axis of symmetry cannot be one of the dissecting diagonals, and there has to be an invariant cell, one of whose diagonals is the axis of symmetry. That means that at one of the fixed vertices (say 1) we have two (reflections of each other) dissecting chords, and the invariant cell is completed by another pair of reflected dissecting chords meeting at the other vertex. An invariant dissection is then determined by an ordered pair of dissections with a total number of $\frac{m-1}{2}$ cells, one to the left of the chord $1\,j$ and the other to the left of the chord $j\,n+1$. So there are s_m such invariant dissections of each of the $m+1$ axes that pass through vertices. For example Fig. 29 shows all the invariant quadrangular dissections of a dodecagon invariant under reflection across the axis 1 7. □

Remark 4.2. The formula for the number of dissections invariant under a rotation has appeared independently in [31][20] as a special case of a more general result about rotation invariant p-angular dissections (see also the paragraph about Sieving Phenomena in Sect. 5). We remark that one can extend the observations in the proof of Theorem 4.1 to the case of p-angular dissections for any $p \geq 3$. This and Theorem 2.12, allow one to obtain the number of p-angular dissections invariant under rotations and reflections for all p.

Let $\mathcal{Q}'_m$ be the set of *unlabeled oriented* quadrangular dissections of the $2(m+2)$-gon, that is quadrangular dissections with m cells up to rotation, and $\widetilde{\mathcal{Q}}_m$ the set of *unlabeled unoriented* quadrangular dissections that is, quadrangular dissections up to rotations and reflections. The number of such dissections q'_m ($\tilde{q}_m$ respectively), is sequence A005034 (A005036 respectively) in the Online Encyclopedia of Integer Sequences [30]. Using Theorem 4.1 and Burnside's lemma we obtain the following explicit formulas:

Theorem 4.3. *The number of quadrangular dissections of a $2(m+1)$-gon up to rotations is*

$$q_m^{'} = \begin{cases} \dfrac{\nu_m}{2(m+1)} + \dfrac{s_m}{2} & \text{if } m \equiv 0 \pmod 2 \\ \dfrac{\nu_m}{2(m+1)} + \dfrac{s_m}{4} + \dfrac{s_{\frac{m-1}{2}}}{2} & \text{if } m \equiv 1 \pmod 4 \\ \dfrac{\nu_m}{2(m+1)} + \dfrac{s_m}{4} & \text{if } m \equiv 3 \pmod 4 \end{cases}$$

The number of quadrangular dissections of a $2(m+1)$-gon up to rotations and reflections is

$$\tilde{q}_m = \begin{cases} \dfrac{\nu_m}{4(m+1)} + \dfrac{3s_m}{4} & \text{if } m \equiv 0 \pmod 2 \\ \dfrac{\nu_m}{4(m+1)} + \dfrac{5s_m}{8} + \dfrac{s_{\frac{m-1}{2}}}{4} & \text{if } m \equiv 1 \pmod 4 \\ \dfrac{\nu_m}{4(m+1)} + \dfrac{5s_m}{8} & \text{if } m \equiv 3 \pmod 4. \end{cases}$$

[20] Thanks to the anonymous referee that brought this work to my attention.

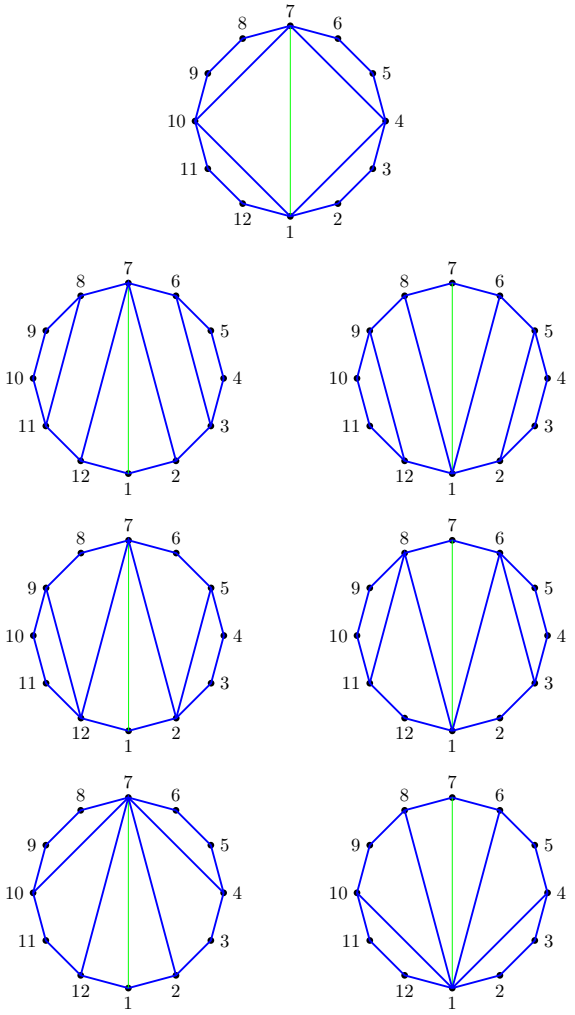

FIGURE 29. Dissections of the dodecagon invariant under reflection across 1 7

Recall that $\mathcal{N}'_m$ stands for the set of oriented unlabeled non-crossing trees with m edges, in other words an element of $\mathcal{N}'_n$ is an orbit of the action of $\langle \kappa^2 \rangle \cong \mathbb{Z}/n$, and $\widetilde{\mathcal{N}}_n$ stands for the set of unoriented unlabeled non-crossing trees, in other words an element of $\widetilde{\mathcal{N}}_n$ is an orbit of the action of the dihedral group $\mathrm{D}_n = \langle \kappa^2, s \rangle$. So Theorem 4.1 allows us to calculate the number of unlabeled oriented and unoriented non-crossing trees as well.

Note that the central element of D_{2n} (rotation by π) belongs to D_n only when m is odd, while its square roots (rotations by $\pm\frac{\pi}{2}$) belong to D_n only when $m \equiv 3 \pmod 4$. It follows that for even m there are no rotation invariant

non-crossing trees, while for odd m only rotation by π has fixed points. So we have the following theorem, proved in [22].[21]

Theorem 4.4. (Noy) *The number of non-crossing trees with n vertices up to rotations is*

$$\nu_m^{'} = \begin{cases} \dfrac{\nu_m}{m+1} & \text{if } m \text{ is even} \\ \dfrac{\nu_m}{m+1} + \dfrac{s_m}{2} & \text{if } m \text{ is odd.} \end{cases}$$

The number of unlabeled non-crossing trees with n vertices is

$$\tilde{\nu}_m = \begin{cases} \dfrac{\nu_m}{2(m+1)} + \dfrac{s_m}{2} & \text{if } m \text{ is even} \\ \dfrac{\nu_m}{2(m+1)} + \dfrac{3s_m}{4} & \text{if } m \text{ is odd.} \end{cases}$$

Finally, we can use a generalization of Burnside's Lemma, the "Counting Lemma" of [26], to count the number of self-dual unlabeled oriented or unoriented trees.

Lemma 4.5. (Robinson's Counting Lemma) *Let G be a group acting on a set X endowed with a permutation r such that $rG = Gr$, so that r is well defined in the orbits of G. Then $N(G, r)$ the number of orbits fixed by r is given by:*

$$N(G, r) = \frac{1}{|G|} \sum_{g \in G} |\{x \in G : grx = x\}| .$$

Applying this theorem in our case with $G = \langle \kappa^2 \rangle \cong \mathbb{Z}/n$ or $G = \langle \kappa^2, s \rangle \cong D_n$ and r the nc-duality, we have

Theorem 4.6. *The number of self-dual unlabeled oriented non-crossing trees with m edges is*

$$s_m^{'} = s_m.$$

The number of self-dual unlabeled unoriented non-crossing trees with m edges is

$$\tilde{s}_m = \begin{cases} s_m & \text{if } m \equiv 0 \pmod 2 \\ \dfrac{s_m + s_{\frac{m-1}{2}}}{2} & \text{if } m \equiv 1 \pmod 4 \\ \dfrac{s_m}{2} & \text{if } m \equiv 3 \pmod 4. \end{cases}$$

Proof. For the case of oriented non-crossing trees we need to look at the fixed points of $\kappa^{2i} r$ for $i = 0, \ldots, n-1$. Each of these elements is a reflection in D_{2n} and so by Theorem 4.1 has s_n fixed elements.

For the case of unoriented unlabeled non-crossing trees, we need in addition to take into account the fixed points of $\kappa^{2i} s\, r$ for $i = 0, \ldots, n-1$. Since $s\, r = \kappa^{-1}$ this means that we have to take into account all the fixed points of odd powers of κ, so the result follows from Theorem 4.1. □

[21] The enumeration of oriented unlabeled trees is not explicitly stated there but a formula can be deduced from the calculations.

It is also of interest to consider *anti-self-dual* non-crossing trees, that is non-crossing-trees $t \in \mathcal{N}'_m$ that satisfy $t^* = \bar{t}$. Since $rs = \kappa$ an anti-self-dual non-crossing tree is fixed by κ^i for some odd power i. So we have

Theorem 4.7. *The number of anti-self-dual non-crossing trees with m vertices is*

$$a_m = \begin{cases} s_m & \text{if } m \equiv 0 \pmod 2 \\ 1 & \text{if } m = 1 \\ s_{\frac{m-3}{2}} & \text{if } m \neq 1 \text{ and } m \equiv 1 \pmod 4 \\ 0 & \text{if } m \equiv 3 \pmod 4. \end{cases}$$

5. Future Directions

5.1. Quadrangular Dissections of Surfaces with Boundary

A bijection ϕ can be defined more generally between appropriately defined *quadrangular dissections* of any surface with boundary and graphs pegged in that surface. Of particular interest is the case where the surface is the annulus, in which case by a simple Euler characteristic argument one sees that the graphs have to be unicyclic, and we plan to explore that direction in a future project.

5.2. Further Connections with Non-crossing Partitions

The $p = 3$ Fuss–Catalan numbers appear in the theory of non-crossing partitions not only as the number of maximal chains "up to commutation" but also as the number of 2-multichains, that is they count the number of pairs $\pi_1 \leq \pi_2$ of non-crossing partitions. More generally, p Fuss–Catalan numbers count the number of p-multichains, that is p-tuples $\pi_1 \leq \pi_2 \leq \cdots \leq \pi_p$ (see [2]). We plan to explore the relation between mind-body duality and the Kreweras complement in that connection.

A further interesting line of future research in connection with non-crossing partitions is to generalize the results of the current work to all finite Coxeter groups.

5.3. Sieving Phenomena

After the research for this project was completed it was brought to my attention that the action of the cyclic group $\mathrm{C}_{2(m+2)}$ on the set of quadrangular dissections with m cells Q_m exhibits an instance of the *Cyclic Sieving Phenomenon* (CSP) (see [25]). Namely, as was proven in [10], if we define the q-analogue of the $p = 3$ Fuss–Catalan numbers by

$$\nu_{m;q} := \frac{1}{(2m+1)_q} \binom{3m}{m}_q,$$

where $(n)_q = 1+q+\cdots+q^{n-1}$, $\binom{n}{k}_q = \frac{(n)_q!}{(k)_q!(n-k)_q!}$, and $(n)_q! = (1)_q(2)_q \ldots (n)_q$, then the triple $\left(\mathcal{Q}_m, \nu_q, \mathrm{C}_{2(m+1)}\right)$ is an instance of CSP[22]. In other words, the

[22] It follows that so is the triple $(\mathcal{N}_m, \nu_q, \mathrm{C}_{m+1})$.

permutation representation $\mathbb{C}[\mathcal{Q}_m]$ of $\mathrm{C}_{2(m+1)}$ can be expressed in the representation ring of $\mathrm{C}_{2(m+1)}$ as $\nu_{m;q}(\omega)$, where ω is a one-dimensional representation that sends the generator of $\mathrm{C}_{2(m+1)}$ to a primitive $2(m+1)$-root of unity. This means that the formulas for the numbers of fixed points of rotations can be obtained by evaluating $\nu_{m;q}$ at roots of unity in $\mathbb{C}$.

Furthermore, it was proven in [31] that for p and m *odd* there is a certain q,t-analogue of Fuss–Catalan numbers, $\mathrm{Cat}_{(p-2)m+1,m}(q,t)$, so that the set $X_{p,m}$ of p-angular dissections of a polygon with m cells exhibits an instance of *Dihedral Sieving Phenomenon* for the natural action of $\mathrm{D}_{(p-2)m+2}$ (see also [24]).

Proving instances of dihedral sieving for actions of dihedral groups of even order with some "naturally defined" polynomials seems to be more complicated. The action of $\mathrm{D}_{2(m+1)}$ on $\mathcal{Q}_m$ seems like a natural place to look for such an instance.

5.4. Self-Dual Maps of the Sphere

Finally, using the connected sum of pegs defined in Section 4.2 of [1], one can "glue" a non-crossing tree and its dual along their common boundary to obtain a self-dual map on the sphere. Not all self-dual maps are obtained with that construction since the resulting graph will have no loops or pendant edges. Furthermore, since the first factors of a pair of dual factorizations agree the resulting graph has at least one bigon. One can rectify that by contracting that bigon into an edge and deleting its dual degree 2 vertex to obtain a rooted self-dual map of the sphere that does not necessarily contain bigons. The following question then seems interesting and open:

Question 5.1. Do all rooted self-dual maps of the sphere without loops arise from gluing together a pair of dual non-crossing trees? If not, characterize those that do.

References

[1] N. Apostolakis. A duality for labeled graphs and factorizations with applications to graph embeddings and Hurwitz enumeration, April 2018. arXiv: 1804.01214.

[2] D. Armstrong. Generalized noncrossing partitions and combinatorics of Coxeter groups. *Mem. Amer. Math. Soc.*, 202(949):x+159, 2009.

[3] Ph. Chassaing and G. Schaeffer. Random planar lattices and integrated super-Brownian excursion. *Probab. Theory Related Fields*, 128(2):161–212, 2004.

[4] J. Cigler. Some remarks on Catalan families. *European J. Combin.*, 8(3):261–267, 1987.

[5] J. Dénes. The representation of a permutation as the product of a minimal number of transpositions, and its connection with the theory of graphs. *Magyar Tud. Akad. Mat. Kutató Int. Közl.*, 4:63–71, 1959.

[6] E. Deutsch, S. Feretić, and M. Noy. Diagonally convex directed polyominoes and even trees: a bijection and related issues. *Discrete Math.*, 256(3):645–654, 2002. LaCIM 2000 Conference on Combinatorics, Computer Science and Applications (Montreal, QC).

[7] The Sage Developers. *SageMath, the Sage Mathematics Software System (Version 8.0)*, 2017. http://www.sagemath.org.

[8] S. Dulucq and J.G. Penaud. Cordes, arbres et permutations. *Discrete Math.*, 117(1-3):89–105, 1993.

[9] J. A. Eidswick. Short factorizations of permutations into transpositions. *Discrete Math.*, 73(3):239–243, 1989.

[10] S.P Eu and T.S. Fu. The cyclic sieving phenomenon for faces of generalized cluster complexes. *Adv. in Appl. Math.*, 40(3):350–376, 2008.

[11] The GAP Group. *GAP – Groups, Algorithms, and Programming, Version 4.7.8*, 2015.

[12] R. L. Graham, D. E. Knuth, and O. Patashnik. *Concrete mathematics*. Addison-Wesley Publishing Company, Reading, MA, second edition, 1994. A foundation for computer science.

[13] J. L. Gross and T. W. Tucker. *Topological Graph Theory*. Dover Books on Mathematics Series. Dover Publications, 1987.

[14] F. Harary, E. M. Palmer, and R. C. Read. On the cell-growth problem for arbitrary polygons. *Discrete Math.*, 11:371–389, 1975.

[15] M. C. Herando. *Complejidad de Estructuras Geométricas y Combinatorias*. PhD thesis, Universitat Politècnica de Catalunya, 1999.

[16] P. Hilton and J. Pedersen. Catalan numbers, their generalization, and their uses. *Math. Intelligencer*, 13(2):64–75, 1991.

[17] D. E. Knuth. Donald Knuth's 20th Annual Christmas Tree Lecture: 3/2–ary Trees. https://www.youtube.com/watch?v=P4AaGQIo0HY, 2014. Accessed 07/13/2018.

[18] S. K. Lando and A. K. Zvonkin. *Graphs on surfaces and their applications*, volume 141 of *Encyclopaedia of Mathematical Sciences*. Springer-Verlag, Berlin, 2004. With an appendix by Don B. Zagier, Low-Dimensional Topology, II.

[19] J. Q. Longyear. Graphs and permutations. In *Graph theory and its applications: East and West (Jinan, 1986)*, volume 576 of *Ann. New York Acad. Sci.*, pages 385–388. New York Acad. Sci., New York, 1989.

[20] P. Moszkowski. A solution to a problem of Dénes: a bijection between trees and factorizations of cyclic permutations. *European J. Combin.*, 10(1):13–16, 1989.

[21] G. Musiker, R. Schiffler, and L. Williams. Positivity for cluster algebras from surfaces. *Adv. Math.*, 227(6):2241–2308, 2011.

[22] M. Noy. Enumeration of noncrossing trees on a circle. *Discrete Math.*, 180(1–3):301 – 313, 1998. Proceedings of the 7th Conference on Formal Power Series and Algebraic Combinatorics.

[23] J. H. Przytycki and A. S. Sikora. Polygon dissections and Euler, Fuss, Kirkman, and Cayley numbers. *J. Combin. Theory Ser. A*, 92(1):68–76, 2000.

[24] S. Rao and J. Suk. Dihedral sieving phenomena. *Discrete Math.*, 343(6):111849, 12, 2020.

[25] V. Reiner, D. Stanton, and D. White. The cyclic sieving phenomenon. *J. Combin. Theory Ser. A*, 108(1):17–50, 2004.

[26] R. W. Robinson. Counting graphs with a duality property. In *Combinatorics (Swansea, 1981)*, volume 52 of *London Math. Soc. Lecture Note Ser.*, pages 156–186. Cambridge Univ. Press, Cambridge-New York, 1981.

[27] K. Rosen. *Discrete Mathematics and Its Applications*. McGraw-Hill, seventh edition, 2012.

[28] F. Ruskey. Generating linear extensions of posets by transpositions. *J. Comb. Theory, Ser. B*, 54(1):77–101, 1992.

[29] G. Schaeffer. *Conjugaison d'arbres et cartes combinatoires aléatoires*. PhD thesis, Université Bordeaux I, 1998.

[30] N. J. A. Sloane, editor. *The On-Line Encyclopedia of Integer Sequences*. Published electronically at https://oeis.org.

[31] Z. Stier, J. Wellman, and Z.X. Xu. Dihedral sieving on cluster complexes, 2019.

Nikos Apostolakis
Department of Mathematics and Computer Science
Bronx Community College, The City University of New York
New York
USA
e-mail: nikolaos.apostolakis@bcc.cuny.edu

Communicated by Matjaz Konvalinka
Received: 12 January 2020.
Accepted: 25 March 2021.